ELSEVIER

Journal of the Mechanics and Physics of Solids
52 (2004) 359–393

JOURNAL OF THE
MECHANICS AND
PHYSICS OF SOLIDS

www.elsevier.com/locate/jmps

A micromechanics-based nonlocal constitutive equation for elastic composites containing randomly oriented spheroidal heterogeneities

Ilaria Monetto[a,*], W.J. Drugan[b]

[a] *Department of Structural and Geotechnical Engineering, University of Genoa, Via Montallegro 1, 16145 Genova, Italy*

[b] *Department of Engineering Physics, University of Wisconsin - Madison, 1500 Engineering Drive, Madison, WI 53706-1687, USA*

Received 17 March 2003; received in revised form 17 June 2003; accepted 24 June 2003

Abstract

A micromechanics-based nonlocal constitutive equation relating the ensemble averages of stress and strain for a matrix containing a random distribution of randomly oriented spheroidal voids or inclusions is derived. The analysis employs J.R. Willis' generalization of the Hashin–Shtrikman variational formulation to random linear elastic composite materials and builds on that of Drugan and Willis (J. Mech. Phys. Solids 44 (1996) 497) and Drugan (J. Mech. Phys. Solids 48 (2000) 1359), who derived completely explicit results for the case of isotropic, nonoverlapping identical spherical inclusions/voids. The model of impenetrable particles employed consists of identical particles with fixed spheroidal shape and random orientation. To facilitate a manageable statistical description, the spheroids are placed within concentric hard "security" spheres. The paper derives three main new results: (i) it is proved within the assumptions just outlined that the effects of inclusion shape and their spatial distribution are separable, for arbitrary inclusion shape (not just spheroids) and arbitrary spatial (statistical) distribution of their security spheres when employing up through two-point statistical information; (ii) closed-form analytical results are obtained from the Verlet–Weis improvement of the Percus–Yevick–Wertheim statistical model of a random distribution of nonoverlapping spherical particles/voids, leading to substantial improvements at higher inclusion/void volume fractions in the nonlocal constitutive equations of Drugan and Willis (1996) and Drugan (2000); (iii) approximate analytical nonlocal constitutive equations are derived for composites consisting of a matrix containing randomly oriented oblate or prolate spheroidal inclusions/voids, using the Verlet–Weis statistical model for the security sphere distribution. Among the specific implications of these new results, it is found that the minimum representative volume element (RVE) size estimate for composites containing spherical inclusions/voids using the Verlet–Weis improvement is significantly larger at higher inclusion/void volume fractions (≈ 0.3–0.64) than the estimates of Drugan and

* Corresponding author. Tel.: +39-010-353-2951; fax: +39-010-353-2534.
E-mail address: monetto@diseg.unige.it (I. Monetto).

doi:10.1016/S0022-5096(03)00103-0

Willis (1996) and Drugan (2000), who used the Percus–Yevick–Wertheim model. Also, deviations in inclusion/void shape from spherical are shown to cause significant modifications to the nonlocal constitutive equations, as evidenced by nontrivial changes in predicted minimum RVE sizes.

Keywords: Nonlocal constitutive equations; Voids and inclusions; Constitutive behavior; Inhomogeneous material

1. Introduction

A classical approach to the mathematical modeling of the constitutive response of elastic composites treats the material as being macroscopically homogeneous with overall properties relating suitable averages of microscopic stress and strain fields over a representative volume element (RVE). The application of such an approach is limited to RVEs sufficiently large compared to the characteristic microstructural length and the length scale of macroscopic field variation that a constant effective modulus tensor gives an acceptably accurate representation of the macroscopic constitutive response. Thus, when the macroscopic or averaged stress and strain fields do not vary slowly with respect to RVE size, more accurate macroscopic constitutive equations are required. Also, estimates of the minimum RVE size are clearly of fundamental importance.

Employing a generalization of the Hashin and Shtrikman (1962a,b) variational formulation to random linear elastic composite materials, due to Willis (1977, 1982, 1983), Drugan and Willis (1996) derived a micromechanics-based nonlocal constitutive equation relating the ensemble averages of stress and strain. With reference to two-phase composites, the nonlocal constitutive equation was derived in closed form for a class of materials consisting of any statistically uniform and isotropic distribution of isotropic phases. The microstructure was described statistically by using up through two-point correlation functions. Nonlocal terms up through the second gradient of ensemble average strain were included. Based on the same variational formulation, a higher-order nonlocal constitutive equation is due to Drugan (2000) who considered nonlocal terms up through the fourth gradient of ensemble-average strain. In both formulations, completely explicit results were derived for the case of a matrix embedding a random distribution of nonoverlapping identical spheres of a different material. Quantitative estimates of minimum RVE size were produced by comparing the magnitude of the nonlocal to local terms in the constitutive equation when ensemble-average strain is spatially varying. Even for high accuracy, these results showed remarkably small minimum RVE sizes for different classes of structural materials and different types of reinforcement: approximately two reinforcement diameters for 5% correction provided by nonlocal to local terms, and 4.5 diameters in the most demanding case studied for 1% correction. Moreover, the minimum RVE size was shown to increase with increasing volume fraction of the embedded phase until a maximum was attained at 0.25–0.35 volume fraction depending on the reinforcement type, after which it starts to decrease slightly.

Well-founded physical and mathematical bases for describing the material's statistics exist for random distributions of nonoverlapping identical spheres. Furthermore, the use of spheres as heterogeneities makes possible the analytical evaluation of some complicated integrals in the nonlocal terms. However, despite the higher level of complexity introduced into the formulation as compared to the case of spheres, treatment of nonspherical particles would permit the preceding theory to be applied to a wider range of practical applications. A good example is particles of spheroidal shape. Short fibers in fiber-reinforced composites may be modeled as spheroids with aspect ratio of the order of 10–100, whereas a body containing penny-shaped cracks may be regarded as a limiting case of a composite with spheroids of aspect ratio tending to zero.

In this paper the analysis builds on that of Drugan and Willis (1996) and Drugan (2000) to derive an explicit nonlocal constitutive equation for a matrix containing a random distribution of nonspherical voids or inclusions. The model of impenetrable heterogeneities employed consists of identical particles with fixed spheroidal shape and random orientation, resulting in macroscopically isotropic behavior. A convenient statistical description of the microstructure is obtained by placing the particles within hard "security" spheres. This assumption is much more restrictive than simply requiring the particles to be nonoverlapping; on the other hand, it makes possible the use of well-known statistical models for the dispersion of security spheres to describe statistically the effective microstructure. As one main new result, it is shown how under all the above assumptions the effects of inclusion shape and their spatial distribution can be separated in the analytical evaluation of the nonlocal correction; this is proved for arbitrary inclusion shape (not just spheroids) and arbitrary statistical distribution of their security spheres, employing up through two-point statistical information. This permits analysis of two statistical mechanics models for the radial distribution function and obtain explicitly, whatever the inclusion/void shape, the related terms describing effects of spatial distribution of inclusions on the nonlocal correction. The first model to be treated was developed by Percus and Yevick (1958) and solved exactly by Wertheim (1963) for a dispersion of hard spheres. The second model is a semi-empirical one proposed by Verlet and Weis (1972), who introduced additional terms to the expression of the radial distribution function to correct defects suffered by the Percus–Yevick–Wertheim model at high densities of spheres. Finally, focusing on spheroidal inclusions/voids, the effects of inclusion shape are shown to involve integrals that are difficult to evaluate analytically except for special cases. In particular, approximate analytical results are obtained for nearly spherical particles, and the limiting cases of matrices weakened/reinforced by cracks/needles are also discussed. Numerical evaluations of these integrals are also performed for a broad range of spheroid aspect ratios.

Two different sets of quantitative results are shown. As verification of the formulation, elastic composites containing spherical particles, already considered by Drugan and Willis (1996) and Drugan (2000), are first considered and previous micromechanics-based variational estimates of minimum RVE size are re-examined by using the improved model for the statistical description of the dispersion of nonoverlapping spheres. As an application of the generalized constitutive model, a new set of quantitative estimates is provided (analytically and numerically) for matrices containing spheroids, for different cases of spheroid shape. In conclusion, the comparison between the two

sets of results permits one to analyze how both shape and type of reinforcement affect minimum RVE size.

2. Nonlocal constitutive equation for two-phase isotropic composites

Employing Willis' (1977, 1982, 1983) generalization of the Hashin and Shtrikman (1962a,b) variational principles, Drugan and Willis (1996) developed a micromechanics-based nonlocal constitutive equation relating the ensemble averages of stress and strain for random linear elastic composite materials comprising firmly bonded homogeneous phases. The analysis dealt with statistically uniform two-phase materials for which an ergodic assumption was made. This hypothesis simply demands that all local configurations available in an ensemble of specimens occur over each specimen of the ensemble. The nonlocal constitutive equation was derived in explicit form for an isotropic distribution of isotropic phases. Their equation comprised only one nonlocal term, in the second gradient of ensemble average strain (the first gradient term vanishes when the phase distribution is isotropic). A higher-order nonlocal constitutive equation is due to Drugan (2000), who considered also the second nonzero nonlocal term, which under the assumptions noted is the fourth gradient of ensemble average strain. This nonlocal constitutive equation has the form

$$\langle\sigma\rangle_{ij}(\mathbf{x}) = \hat{L}_{ijkl}\langle e\rangle_{kl}(\mathbf{x}) + \hat{L}^{(1)}_{ijklmn}\frac{\partial^2\langle e\rangle_{kl}(\mathbf{x})}{\partial x_m\partial x_n} + \hat{L}^{(2)}_{ijklmnop}\frac{\partial^4\langle e\rangle_{kl}(\mathbf{x})}{\partial x_m\partial x_n\partial x_o\partial x_p}, \tag{2.1}$$

where angle brackets denote ensemble average; σ_{ij} and e_{ij} are the stress and infinitesimal strain components; $\mathbf{x}$ is the position vector; $\hat{L}_{ijkl}, \hat{L}^{(1)}_{ijklmn}$ and $\hat{L}^{(2)}_{ijklmnop}$ are isotropic tensors whose components depend on the matrix elastic moduli, the shape, elastic properties and statistical distribution of the phases, as well as on the choice of the homogeneous comparison material. The detailed derivation of these tensors can be found in the references just cited; here, it is of interest to recall only their final forms for the specific choice of the comparison moduli equal to the matrix moduli, used in the subsequent analysis. As justified by Drugan (2000), this is the optimal choice to minimize the nonlocal correction to the standard constant-effective-modulus constitutive model.

In this case the local fourth-order tensor is

$$\hat{L}_{ijkl} = (\kappa + c_1\kappa_B)\delta_{ij}\delta_{kl} + (\mu + c_1\mu_B)(\delta_{ik}\delta_{jl} + \delta_{il}\delta_{jk} - 2/3\delta_{ij}\delta_{kl}), \tag{2.2}$$

where δ_{ij} is the Kronecker delta, c_1 is the volume concentration of inclusions having bulk modulus κ_1 and shear modulus μ_1, κ and μ are the matrix bulk and shear moduli. Having defined $\delta\kappa = \kappa_1 - \kappa$ and $\delta\mu = \mu_1 - \mu$, constants, κ_B and μ_B in Eq. (2.2) are:

$$\kappa_B = \frac{\delta\kappa(3\kappa + 4\mu)}{4\mu + 3(\kappa_1 - c_1\delta\kappa)}, \qquad \mu_B = \frac{5\mu\delta\mu(3\kappa + 4\mu)}{\mu(9\kappa + 8\mu) + 6(\kappa + 2\mu)(\mu_1 - c_1\delta\mu)}. \tag{2.3}$$

The sixth-order nonlocal tensor can be written as

$$\hat{L}^{(1)}_{ijklmn} = \frac{c_1(1 - c_1)}{2}[B_{ijpq}\Gamma_{pqst,mn}B_{stkl}], \tag{2.4}$$

where

$$B_{ijkl} = \kappa_B \delta_{ij}\delta_{kl} + \mu_B(\delta_{ik}\delta_{jl} + \delta_{il}\delta_{jk} - 2/3\delta_{ij}\delta_{kl}), \tag{2.5}$$

$$\Gamma_{ijkl,mn} = (Q_{ijklmn} - \delta_{mn}P_{ijkl}) \left[\int_0^\infty h(r) r \, \mathrm{d}r\right], \tag{2.6}$$

$h(r)$ is the two-point correlation function for the dispersion of inclusions and having defined

$$P_{ijkl} = -\frac{3\kappa + \mu}{15\mu(3\kappa + 4\mu)} \delta_{ij}\delta_{kl} + \frac{3(\kappa + 2\mu)}{10\mu(3\kappa + 4\mu)} (\delta_{ik}\delta_{jl} + \delta_{il}\delta_{jk}), \tag{2.7}$$

$$Q_{ijklmn} = \frac{3(3\kappa + 8\mu)}{140\mu(3\kappa + 4\mu)} I^{(6)}_{ijklmn} - \frac{1}{20\mu}\left[\delta_{ij}I^{(4)}_{klmn} + \delta_{kl}I^{(4)}_{ijmn} - \delta_{mn}I^{(4)}_{ijkl}\right], \tag{2.8}$$

together with

$$I^{(4)}_{ijkl} = \delta_{ij}\delta_{kl} + \delta_{ik}\delta_{jl} + \delta_{il}\delta_{jk}, \tag{2.9}$$

$$I^{(6)}_{ijklmn} = \delta_{ij}I^{(4)}_{klmn} + \delta_{ik}I^{(4)}_{jlmn} + \delta_{il}I^{(4)}_{jkmn} + \delta_{im}I^{(4)}_{jkln} + \delta_{in}I^{(4)}_{jklm}. \tag{2.10}$$

Finally, the eighth-order nonlocal tensor is given by

$$\hat{L}^{(2)}_{ijklmnop} = \frac{c_1(1-c_1)}{24}\left[B_{ijqr}(6(1-c_1)\Gamma_{qrst,mn}B_{stuv}\Gamma_{uvwx,op} - \Gamma_{qrwx,mnop})B_{wxkl}\right], \tag{2.11}$$

where tensors $\mathbf{B}$ and $\mathbf{\Gamma}_{,mn}$ are given by Eqs. (2.5) and (2.6), while

$$\Gamma_{ijkl,mnop} = \frac{1}{2}(3P_{ijkl}\delta_{mn}\delta_{op} - 6Q_{ijklmn}\delta_{op} + R_{ijklmnop}) \left[\int_0^\infty h(r) r^3 \, \mathrm{d}r\right], \tag{2.12}$$

having defined

$$R_{ijklmnop} = \frac{1}{28\mu}\left(\delta_{jk}I^{(6)}_{ilmnop} + \delta_{ik}I^{(6)}_{jlmnop} + \delta_{jl}I^{(6)}_{ikmnop} + \delta_{il}I^{(6)}_{jkmnop}\right) - \frac{3\kappa + \mu}{63\mu(3\kappa + 4\mu)} I^{(8)}_{ijklmnop}, \tag{2.13}$$

together with

$$I^{(8)}_{ijklmnop} = \delta_{ij}I^{(6)}_{klmnop} + \delta_{ik}I^{(6)}_{jlmnop} + \delta_{il}I^{(6)}_{jkmnop} + \delta_{im}I^{(6)}_{jklnop} + \delta_{in}I^{(6)}_{jklmop} + \delta_{io}I^{(6)}_{jklmnp} + \delta_{ip}I^{(6)}_{jklmno}. \tag{2.14}$$

Note that the entire nonlocal constitutive equation, (2.1) with Eqs. (2.2)–(2.14), is completely explicit except for the evaluation of the two radial integrals in Eqs. (2.6)

and (2.12):

$$H = \int_0^\infty h(r) r \, \mathrm{d}r, \tag{2.15}$$

$$\bar{H} = \int_0^\infty h(r) r^3 \, \mathrm{d}r. \tag{2.16}$$

In order to determine these, the two-point correlation function $h(r)$ must be specified. Thus, the two-phase composite, already specialized to an isotropic distribution of isotropic phases, must be further specialized to the specific case of inclusion shape and distribution under consideration. Random distributions of nonoverlapping identical spheres, for which well-founded physical and mathematical bases for describing the material's statistics exist, were previously considered by Drugan and Willis (1996) and Drugan (2000), who derived completely explicit results. Here, attention is focused on the case of nonspherical inclusions, as well as on improving prior results for spherical inclusions/voids by use of a more accurate statistical model. Namely, a random distribution of nonoverlapping randomly oriented identical spheroids in a matrix of different material is considered. The next section deals with the details of the evaluation of H and $\bar{H}$ for such a dispersion.

3. Two-point statistics for isotropic distributions of nonoverlapping randomly oriented identical inclusions/voids

The model of impenetrable particles considered here consists of nonoverlapping identical inclusions/voids of characteristic length $2a$ having random orientations. The spatial location and orientation of each inclusion/void are specified by the location $\mathbf{z} \in \Re^3$ of the center and by the unit vector $\boldsymbol{\omega} \in \Omega$ directed along the characteristic semi-axis a, the unit hemi-sphere in $\Re^3$ being denoted by Ω. The related indicator function $\chi_s(\mathbf{x}-\mathbf{z};\boldsymbol{\omega}) = 1$ when $\mathbf{x}-\mathbf{z}$ lies in the domain of the reference inclusion/void, and $=0$ otherwise.

As suggested by Markov (1998), a convenient statistical description of such a random array employs the formalism of marked sets of random points, treating the orientation of each inclusion/void as the mark of its center point, and defines by $\hat{p}_k$ the multi-point probability densities such that

$$\mathrm{d}P = \hat{p}_k(\mathbf{z}_1,\ldots,\mathbf{z}_k;\boldsymbol{\omega}_1,\ldots,\boldsymbol{\omega}_k)\,\mathrm{d}\mathbf{z}_1\ldots\mathrm{d}\mathbf{z}_k\,\mathrm{d}\boldsymbol{\omega}_1\ldots\mathrm{d}\boldsymbol{\omega}_k \tag{3.1}$$

is the probability that k center points lie simultaneously in the vicinities $\mathrm{d}\mathbf{z}_1,\ldots,\mathrm{d}\mathbf{z}_k$ of $\mathbf{z}_1,\ldots,\mathbf{z}_k$, respectively, whereas the related marks lie simultaneously in the vicinities $\mathrm{d}\boldsymbol{\omega}_1,\ldots,\mathrm{d}\boldsymbol{\omega}_k$ of $\boldsymbol{\omega}_1,\ldots,\boldsymbol{\omega}_k$. Preventing particles from overlapping introduces a higher level of complexity to the definition of functions $\hat{p}_k$, already quite difficult to determine. For analytical tractability, we make two simplifying assumptions: (i) particle spatial location and orientation are statistically independent, implying the factorization $\hat{p}_k(\mathbf{z}_1,\ldots,\mathbf{z}_k;\boldsymbol{\omega}_1,\ldots,\boldsymbol{\omega}_k) = p_k(\mathbf{z}_1,\ldots,\mathbf{z}_k)F_k(\boldsymbol{\omega}_1,\ldots,\boldsymbol{\omega}_k)$; (ii) spatial orientation of each

particle is independent of that of all others, implying factorization of the mark density functions $F_k(\boldsymbol{\omega}_1,\ldots,\boldsymbol{\omega}_k)=F_1(\boldsymbol{\omega}_1)F_2(\boldsymbol{\omega}_2)\ldots F_k(\boldsymbol{\omega}_k)$. We further assume no long-range order (Willis, 1982), meaning that $p_k(\mathbf{z}_1,\ldots,\mathbf{z}_k)\to n^k$ when $|z_j-z_i|\to\infty$ for all $i\neq j$, $k\geqslant 2$, where n is the number density of the inclusions/voids. Finally, one implication of our assumption of statistical uniformity is that $F_i(\boldsymbol{\omega}_i)$ with $i=1,\ldots,k$ reduces to a constant, meaning that $F_i(\boldsymbol{\omega}_i)=1/2\pi$ because of the requirement $\int_\Omega F_i(\boldsymbol{\omega}_i)\,\mathrm{d}\boldsymbol{\omega}_i=1$. Employing this and the factorizations just noted show that the probability density functions have the simplified forms:

$$\hat{p}_k(\mathbf{z}_1,\ldots,\mathbf{z}_k;\boldsymbol{\omega}_1,\ldots,\boldsymbol{\omega}_k)=\left(\frac{1}{2\pi}\right)^k p_k(\mathbf{z}_1,\ldots,\mathbf{z}_k). \tag{3.2}$$

Within an up-through two-point statistical description of the isotropic distribution considered, the probability density functions of interest are, employing Eq. (3.2) and enforcing all our statistical uniformity, ergodicity and isotropy assumptions:

$$\hat{p}_1(\mathbf{z};\boldsymbol{\omega})=\frac{n}{2\pi}\quad\text{and}\quad\hat{p}_2(\mathbf{z}_1,\mathbf{z}_2;\boldsymbol{\omega}_1,\boldsymbol{\omega}_2)=\frac{1}{4\pi^2}\,p_2(|\mathbf{z}_2-\mathbf{z}_1|). \tag{3.3}$$

Under the above assumptions, a sufficient condition for nonoverlapping is: $p_2=0$ for $|\mathbf{z}_2-\mathbf{z}_1|<2a$. In fact, if the centers of two heterogeneities are closer than $2a$, their orientations cannot be mutually independent unless they are allowed to overlap. This leads one, for simplicity and to permit analytical representation, to consider the inclusions/voids as placed within concentric "security" spheres of radius a, and to refer to this random set of spheres to describe the statistics for the dispersion of the inclusion/void centers, so that the second equation of Eq. (3.3) becomes

$$\hat{p}_2(\mathbf{z}_1,\mathbf{z}_2;\boldsymbol{\omega}_1,\boldsymbol{\omega}_2)=\frac{n^2}{4\pi^2}\,g(|\mathbf{z}_2-\mathbf{z}_1|), \tag{3.4}$$

having introduced the radial distribution function g for the dispersion of hard identical security spheres. Note that the number density of the security spheres equals n, whereas the volume fraction $c_a=nV_a$ of the security spheres differs from $c_1=nV_s$ of the inclusions/voids, V_a and V_s denoting the security sphere and inclusion/void volumes, respectively.

Now, recall that the two-point correlation function $h(r)$ for a statistically uniform two-phase material consisting of an isotropic distribution of phases satisfies the relation (Willis, 1982)

$$h(r)=\frac{1}{c_1(1-c_1)}\,[P_2(r)-c_1^2], \tag{3.5}$$

where $P_2(r)$ is the probability that two points $\mathbf{x}_1$ and $\mathbf{x}_2$ separated by $r=|\mathbf{x}_2-\mathbf{x}_1|$ fall simultaneously in the inclusions/voids. There are only two possibilities for such an event: either both $\mathbf{x}_1$ and $\mathbf{x}_2$ fall in the same inclusion/void (Event A) or $\mathbf{x}_1$ and $\mathbf{x}_2$ fall in two different inclusions/voids having in general different orientations (Event B). Let P_A and P_B be the probabilities of Events A and B, respectively. The addition law for probabilities then gives

$$P_2(r)=P_A(r)+P_B(r). \tag{3.6}$$

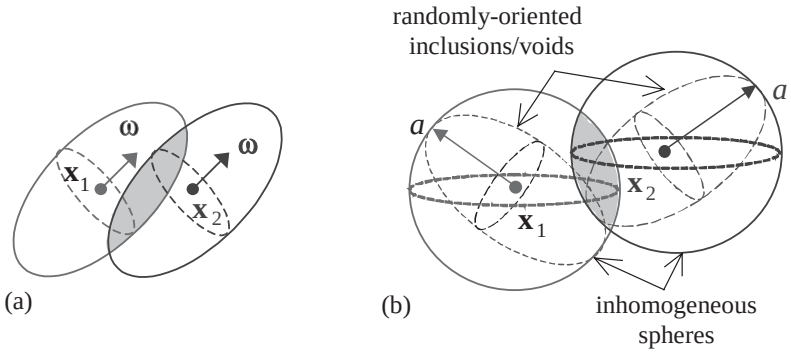

Fig. 1. Locus of the centers of inclusions/voids containing two given points $\mathbf{x}_1$ and $\mathbf{x}_2$: (a) event A; (b) event B.

Using the first equation of (3.3), the probability of Event A is

$$P_A(r) = n\left\{\frac{1}{2\pi}\int_{\Omega}\left[\int_{\Re^3}\chi_s(\mathbf{x}_1-\mathbf{z};\boldsymbol{\omega})\chi_s(\mathbf{x}_2-\mathbf{z};\boldsymbol{\omega})\,\mathrm{d}\mathbf{z}\right]\mathrm{d}\boldsymbol{\omega}\right\}. \tag{3.7}$$

In this expression, notice that the total $\mathbf{z}$-space integral (between square brackets) is the intersection volume of two aligned inclusions/voids centered at $\mathbf{x}_1$ and $\mathbf{x}_2$, respectively (Fig. 1a), whereas the surface integral over the unit hemi-sphere Ω (between braces) takes the average of such an intersection volume over all orientations. It is straightforward that the final result is a function of r that $=0$ when $r > 2a$ and can be written for compactness as

$$P_A(r) = nV_a f_A(\rho)\chi_{2a}(r) = c_a f_A(\rho)\chi_{2a}(r), \tag{3.8}$$

where $\chi_{2a}(r)$ is the indicator function of a sphere of radius $2a$ ($\chi_{2a}(r)=1$ when $r \leqslant 2a$, and $=0$ otherwise) and hereafter, unless specified otherwise, $\rho = r/a$; whereas function f_A depends on the specific shape of the inclusions/voids. In Section 5 the general definition of f_A is given for oblate and prolate spheroidal inclusions/voids, while explicit expressions are provided in Appendix A.

Using Eq. (3.4), the probability of Event B is

$$P_B(r) = n^2\int_{\Re^3} g(|\mathbf{z}'|)\left\{\int_{\Re^3}\left[\frac{1}{2\pi}\int_{\Omega}\chi_s(\mathbf{x}_1-\mathbf{z};\boldsymbol{\omega})\,\mathrm{d}\boldsymbol{\omega}\right]\left[\frac{1}{2\pi}\int_{\Omega}\chi_s(\mathbf{x}_2-\mathbf{z}'-\mathbf{z};\boldsymbol{\omega}')\,\mathrm{d}\boldsymbol{\omega}'\right]\mathrm{d}\mathbf{z}\right\}\mathrm{d}\mathbf{z}'. \tag{3.9}$$

It is worthwhile to note first that Eq. (3.9) reduces to $P_B = c_1^2$ for $g(|\mathbf{z}'|)=1$. Secondly, each surface integral over the unit hemi-sphere Ω (between square brackets) returns a geometrical quantity, that is, the sphere described by an inclusion/void varying its orientation over Ω. Such a sphere of radius a is statistically inhomogeneous and equivalent to an inclusion/void randomly oriented. Let S denote a spherical shell of radius r,

concentric with the reference inclusion/void. Varying r from 0 to a, the statistical density $\gamma(r)$ of the equivalent inhomogeneous sphere is defined as the ratio between the portion of S falling into the inclusion/void and the total surface of S. Finally, the total $\mathbf{z}$-space integral (between braces) in Eq. (3.9) represents the intersection volume of two such inhomogeneous spheres centered at $\mathbf{x}_1$ and $\mathbf{x}_2$, respectively (Fig. 1b), which results in a radial function defined from 0 to $2a$. Analogously with Eq. (3.8), Eq. (3.9) can then be written for compactness as

$$P_B(r) = nc_a \int_{\Re^3} f_B(\rho^*)\chi_{2a}(|\mathbf{x}_2 - \mathbf{x}_1 - \mathbf{z}'|)g(|\mathbf{z}'|)\,\mathrm{d}\mathbf{z}', \tag{3.10}$$

where here $\rho^* = |\mathbf{x}_2 - \mathbf{x}_1 - \mathbf{z}'|/a$ and function f_B must be specialized to the specific shape of the inclusions/voids. More details about the derivation of f_B are discussed in Sections 5 and 6 for particles of oblate and prolate spheroidal shape.

Verification for Eqs. (3.8) and (3.9) can be found in Quintanilla (1999), who first used the model of impenetrable particles within security spheres to derive the matrix probability functions in random media. However, he evaluated numerically the total $\mathbf{z}$- and $\mathbf{z}'$-space double integral in Eq. (3.9) by employing the Fourier transform of the density function and the standard Percus–Yevick–Wertheim approximation for the radial distribution function, restricting the analysis to particles of ellipsoidal shape. In contrast, a main goal of the present paper is to produce explicit analytical results for the two-point correlation function and the two radial integrals H and $\bar{H}$, and thus to obtain a more versatile constitutive model. Further, we will prove within the assumptions outlined above that the effects of inclusion shape and their spatial distribution are separable, for arbitrary inclusion shape and arbitrary statistical distribution of their security sphere centers when employing up through two-point statistical information. Finally, we will incorporate the Verlet–Weis improvement to the standard Percus–Yevick–Wertheim approximation.

In order to do this, a convenient representation for $g(r)$ ($g(r) = 0$ for $r < 2a$) is the form suggested by Markov and Willis (1998):

$$g(r) = 1 - \chi_{2a}(r) + \int_{2a}^{\infty} [g(y) - 1]\,\frac{\mathrm{d}}{\mathrm{d}y}\,(\chi_y(r))\,\mathrm{d}y, \tag{3.11}$$

where χ_y is the indicator function of a sphere of radius $y \geqslant 2a$: $\chi_y(r) = 1$ when $r \leqslant y$, and $=0$ otherwise. Using Eq. (3.11), recalling that $P_B = c_1^2$ for $g = 1$ and interchanging the order of integration, Eq. (3.10) can be written as

$$\begin{aligned} P_B(r) = c_1^2 &- nc_a \left[\int_{\Re^3} f_B(\rho^*)\chi_{2a}(|\mathbf{x}_2 - \mathbf{x}_1 - \mathbf{z}'|)\chi_{2a}(|\mathbf{z}'|)\mathrm{d}\mathbf{z}'\right] \\ &+ nc_a \int_{2a}^{\infty} [g(y) - 1] \\ &\times \frac{\mathrm{d}}{\mathrm{d}y}\left[\int_{\Re^3} f_B(\rho^*)\,\chi_{2a}(|\mathbf{x}_2 - \mathbf{x}_1 - \mathbf{z}'|)\chi_y(|\mathbf{z}'|)\,\mathrm{d}\mathbf{z}'\right]\,\mathrm{d}y. \end{aligned} \tag{3.12}$$

Alternatively, having noted that both bracketed terms are convolutions, one obtains

$$P_B(r) = c_1^2 - nc_a(f_B\chi_{2a} * \chi_{2a})(r) + nc_a \int_{2a}^{\infty} [g(y) - 1] \frac{\mathrm{d}}{\mathrm{d}y} (f_B\chi_{2a} * \chi_y)(r)\, \mathrm{d}y. \tag{3.13}$$

Finally, using Eqs. (3.8) and (3.13) in Eq. (3.6) and the result in Eq. (3.5) gives the following new and compact single-integral representation for the two-point correlation function for the dispersion of nonoverlapping randomly oriented identical inclusions/voids of arbitrary shape

$$h(r) = \frac{c_a}{c_1(1-c_1)} \left[f_A(\rho)\chi_{2a}(r) - n(f_B\chi_{2a}^* \chi_{2a})(r) \right] + \frac{nc_a}{c_1(1-c_1)} \int_{2a}^{\infty} [g(y) - 1] \frac{\mathrm{d}}{\mathrm{d}y} (f_B\chi_{2a} * \chi_y)(r)\, \mathrm{d}y = h^{ws}(r) + h^*(r), \tag{3.14}$$

which is a generalization of the result obtained by Markov and Willis (1998) for dispersions of nonoverlapping spheres. The formula can be conveniently split into two parts: $h^{ws}(r)$ is an approximation corresponding to the case of *well-stirred* dispersions, characterized by no two-particle correlations outside the sphere of radius $2a$ within which the centers of two particles cannot fall due to the fact that overlapping is forbidden ($g(r) = 0$ for $r < 2a$ and $g(r) = 1$ for $r \geqslant 2a$); $h^*(r)$ is a correction term to defects suffered by the well-stirred approximation for $c_a > 1/8$.

The model of impenetrable particles introduced above is now employed to evaluate analytically the two radial integrals H and $\bar{H}$, defined in Eqs. (2.15) and (2.16), of the two-point correlation function $h(r)$:

$$H = \int_0^{\infty} h(r) r\, \mathrm{d}r = a^2 \int_0^{\infty} h(\rho)\rho\, \mathrm{d}\rho = a^2 \int_0^{\infty} [h^{ws}(\rho) + h^*(\rho)]\rho\, \mathrm{d}\rho, \tag{3.15}$$

$$\bar{H} = \int_0^{\infty} h(r) r^3\, \mathrm{d}r = a^4 \int_0^{\infty} h(\rho)\, \rho^3\, \mathrm{d}\rho = a^4 \int_0^{\infty} [h^{ws}(\rho) + h^*(\rho)]\rho^3\, \mathrm{d}\rho. \tag{3.16}$$

Using the two-point correlation function (3.14), the integrals appearing in the last of Eqs. (3.15) and (3.16) can be rewritten for compactness as

$$\int_0^{\infty} \rho^m h^{ws}(\rho)\, \mathrm{d}\rho = \frac{c_a}{c_1(1-c_1)} \left\{ \int_0^2 \rho^m f_A(\rho)\, \mathrm{d}\rho - n \int_0^{\infty} \rho^m (f_B\chi_{2a} * \chi_{2a})(\rho)\, \mathrm{d}\rho \right\}, \tag{3.17}$$

$$\int_0^{\infty} \rho^m h*(\rho)\, \mathrm{d}\rho = \frac{nc_a}{c_1(1-c_1)} \int_0^{\infty} \rho^m \left[\int_2^{\infty} [g(\xi) - 1] \frac{\mathrm{d}}{\mathrm{d}\xi} (f_B\chi_{2a} * \chi_{\xi a})(\rho)\, \mathrm{d}\xi \right] \mathrm{d}\rho, \tag{3.18}$$

where $\xi = y/a$. Setting $m = 1$ in Eqs. (3.17) and (3.18) provides contributions to H, whereas $m = 3$ corresponds to terms appearing in the expression of $\bar{H}$.

As regards integrals which involve function f_B in both Eqs. (3.17) and (3.18), more explicit results can be obtained based on simple geometrical interpretations. The key point in the evaluation of these integrals is that their integrands are convolutions and represent geometrically intersection volumes of two spheres whose centers are separated by r: the first sphere, of radius $2a$, is inhomogeneous with density f_B; the second sphere, of radius $y = \xi a$, is homogeneous ($\xi = 2$ returns the convolution in the last integral of Eq. (3.17), while $\xi \geqslant 2$ returns the convolution in Eq. (3.18)). Notice that such intersection volumes admit representations (B.7) and (B.8) specialized for $b = 2a$, $\bar{b} = \xi a$ and $f = f_B$. Thus, as regards the last integral in the well-stirred approximation (3.17) where $y = 2a$, it is straightforward to show that

$$\int_0^\infty \rho^m (f_B \chi_{2a} * \chi_{2a})(\rho)\,\mathrm{d}\rho = \frac{3}{4} V_a \left\{ \int_2^4 \rho^{m-1} \left[\int_{\rho-2}^2 \delta[4-(\rho-\delta)^2] f_B(\delta)\,\mathrm{d}\delta \right] \mathrm{d}\rho \right\} + 3V_a \left\{ \int_0^2 \rho^m \left[\int_0^{2-\rho} \delta^2 f_B(\delta)\,\mathrm{d}\delta + \int_{2-\rho}^2 \frac{\delta[4-(\rho-\delta)^2]}{4\rho} f_B(\delta)\,\mathrm{d}\delta \right] \mathrm{d}\rho \right\}. \tag{3.19}$$

Since $f_B(\delta)$ is not known explicitly unless the particle shape is specified, let us interchange the order of integration of all the integrals and evaluate first the ρ-integral. Combining terms, Eq. (3.19) finally reduces to

$$\int_0^\infty \rho^m (f_B \chi_{2a} * \chi_{2a})(\rho)\,\mathrm{d}\rho = \frac{V_a}{40} \int_0^2 f_B(\delta)\delta^2 \left[10(3-m)(12-\delta^2) + (m-1)(240+40\delta^2-\delta^4) \right] \mathrm{d}\delta, \tag{3.20}$$

which is a simple radial integral of function f_B and thus depends only on the inclusion/void shape. On the other hand, as regards the double integral in Eq. (3.18), the first derivative with respect to the radius of the homogeneous sphere of the intersection volume just mentioned is involved. This admits the representation (B.9) specialized for $b = 2a$, $\bar{b} = \xi a$ and $f = f_B$. Thus, we have

$$\int_0^\infty \rho^m \left[\int_2^\infty [g(\xi)-1] \frac{\mathrm{d}}{\mathrm{d}\xi} (f_B \chi_{2a} * \chi_{\xi a})(\rho)\,\mathrm{d}\xi \right] \mathrm{d}\rho = \frac{3V_a}{2} \left\{ \int_2^\infty [g(\xi)-1] \left[\int_{\xi-2}^{\xi} \rho^{m-1} \left(\int_{\xi-\rho}^2 \delta\xi f_B(\delta)\,\mathrm{d}\delta \right) \mathrm{d}\rho + \int_{\xi}^{\xi+2} \rho^{m-1} \left(\int_{\rho-\xi}^2 \delta\xi f_B(\delta)\,\mathrm{d}\delta \right) \mathrm{d}\rho \right] \mathrm{d}\xi \right\}. \tag{3.21}$$

Interchanging the order of integration of the ρ- and δ-integrals, evaluating the ρ-integral and combining terms, Eq. (3.21) finally reduces to

$$\int_0^\infty \rho^m \left[\int_2^\infty [g(\xi)-1]\frac{\mathrm{d}}{\mathrm{d}\xi}(f_B\chi_{2a} * \chi_{\xi a})(\rho)\,\mathrm{d}\xi\right]\mathrm{d}\rho$$
$$= \frac{V_a}{2}\left[\int_2^\infty \xi[g(\xi)-1]\,\mathrm{d}\xi\right]\left[\int_0^2 f_B(\delta)[3(3-m)\delta^2+(m-1)\delta^4]\,\mathrm{d}\delta\right]$$
$$+\frac{3V_a}{2}(m-1)\left[\int_2^\infty \xi^3[g(\xi)-1]\,\mathrm{d}\xi\right]\left[\int_0^2 \delta^2 f_B(\delta)\,\mathrm{d}\delta\right], \tag{3.22}$$

where observe that the ξ- and δ-integrals are mutually independent, as grouped above, and can thus be evaluated separately.

Finally, introducing Eqs. (3.20) and (3.22) into Eqs. (3.17) and (3.18) and the results into Eqs. (3.15) and (3.16), H and $\bar{H}$ assume the forms

$$H = \frac{c_a a^2}{c_1(1-c_1)}\left\{\mathfrak{F}_A + c_a\left[\int_0^2 \frac{\rho^2(\rho^2-12)}{2} f_B(\rho)\,\mathrm{d}\rho\right.\right.$$
$$\left.\left.+3\,\mathfrak{X}\int_0^2 \rho^2 f_B(\rho)\,\mathrm{d}\rho\right]\right\}, \tag{3.23}$$

$$\bar{H} = \frac{c_a a^4}{c_1(1-c_1)}\left\{\bar{\mathfrak{F}}_A + \frac{c_a}{20}\left[\int_0^2 \rho^2(\rho^4-40\rho^2-240) f_B(\rho)\,\mathrm{d}\rho\right]\right.$$
$$\left.+c_a\left[\mathfrak{X}\int_0^2 \rho^4 f_B(\rho)\,\mathrm{d}\rho + 3\bar{\mathfrak{X}}\int_0^2 \rho^2 f_B(\rho)\,\mathrm{d}\rho\right]\right\}, \tag{3.24}$$

having defined

$$\mathfrak{F}_A = \int_0^2 \rho\, f_A(\rho)\,\mathrm{d}\rho, \quad \bar{\mathfrak{F}}_A = \int_0^2 \rho^3 f_A(\rho)\,\mathrm{d}\rho, \tag{3.25}$$

and

$$\mathfrak{X} = \int_2^\infty \xi[g(\xi)-1]\,\mathrm{d}\xi, \quad \bar{\mathfrak{X}} = \int_2^\infty \xi^3[g(\xi)-1]\,\mathrm{d}\xi, \tag{3.26}$$

which straightforwardly vanish under the assumption of a well-stirred distribution ($g(r) = 1$ for $r \geqslant 2a$).

Physical and analytical implications of the approach followed here in the evaluation of nonlocal corrections are now discussed. This approach has permitted separation of the effects of inclusion shape and spatial distribution, regardless of the specific inclusion/void shape. Integrals $\mathfrak{F}_A$, $\bar{\mathfrak{F}}_A$ as well as all radial integrals involving function f_B describe shape effects. As an example, in Sections 5 and 6 randomly oriented oblate and prolate spheroids, for which $\mathfrak{F}_A, \bar{\mathfrak{F}}_A$ are known analytically, whereas evaluation of

the other integrals cannot be obtained in closed form except for particular cases, are considered. Section 5 deals also with the special case of spheres for which completely explicit expressions are derived, whereas some approximate results for randomly oriented spheroids of particular aspect ratios are discussed in Section 6. As regards the spatial distribution of inclusions, this affects the nonlocal correction only through integrals $\mathfrak{X}$ and $\bar{\mathfrak{X}}$ which are simple integrals of the radial distribution function for the dispersion of security sphere centers. Thus, completely explicit expressions for $\mathfrak{X}$ and $\bar{\mathfrak{X}}$ require knowledge of g. In the next section two statistical mechanics models for the radial distribution function are analyzed and the related integrals $\mathfrak{X}$ and $\bar{\mathfrak{X}}$ are obtained explicitly.

4. Effects of spatial distribution of inclusions on the nonlocal correction

As proved in the previous section, the effects of the statistical distribution of heterogeneities are described, whatever their shape, by the two integrals $\mathfrak{X}$ and $\bar{\mathfrak{X}}$ of the radial distribution function g for the dispersion of their security spheres defined by Eqs. (3.26) which admit also the following representations, recalling that $g(\rho)=0$ for $\rho<2$ since security spheres are not allowed to overlap

$$\mathfrak{X}=\int_2^\infty \rho[g(\rho)-1]\,\mathrm{d}\rho=\int_0^2 \rho\,\mathrm{d}\rho+\lim_{s\to 0}\left[\int_0^\infty \rho[g(\rho)-1]\mathrm{e}^{-s\rho}\,\mathrm{d}\rho\right]$$
$$=2+\lim_{s\to 0} f(s), \tag{4.1}$$

and, following a similar approach

$$\bar{\mathfrak{X}}=\int_2^\infty \rho^3[g(\rho)-1]\,\mathrm{d}\rho=4+\lim_{s\to 0}\left[\int_0^\infty \rho^3[g(\rho)-1]\mathrm{e}^{-s\rho}\,\mathrm{d}\rho\right]$$
$$=4+\lim_{s\to 0}\frac{\mathrm{d}^2 f(s)}{\mathrm{d}s^2}, \tag{4.2}$$

having defined

$$f(s)=\int_0^\infty \rho g(\rho)\mathrm{e}^{-s\rho}\,\mathrm{d}\rho-\frac{1}{s^2}. \tag{4.3}$$

Within the framework of classical fluid theory, theoretical and experimental investigation of the radial distribution function has been the subject of many studies, resulting in various approximate integral equations for the radial distribution function of a system of interacting particles disordered with respect to position. The best known of these is due to Percus and Yevick (1958) which Wertheim (1963) solved as a closed-form Laplace transform for the case of hard identical spheres (*the hard-sphere fluid model*)

$$\int_0^\infty \rho g(\rho;c_a)\mathrm{e}^{-s\rho}\,\mathrm{d}\rho=\frac{8sL(2s;c_a)}{12c_a[L(2s;c_a)+M(2s;c_a)\,\mathrm{e}^{2s}]}, \tag{4.4}$$

where

$$L(t;\eta) = 12\eta\left[\left(1+\frac{\eta}{2}\right)t + (1+2\eta)\right], \tag{4.5}$$

$$M(t;\eta) = (1-\eta)^2 t^3 + 6\eta(1-\eta)t^2 + 18\eta^2 t - 12\eta(1+2\eta).$$

Using this exact solution as the statistical model for the radial distribution function, $f(s)$ becomes

$$f(s) = \frac{8sL(2s;c_a)}{12c_a[L(2s;c_a) + M(2s;c_a)\mathrm{e}^{2s}]} - \frac{1}{s^2}, \tag{4.6}$$

from which integrals $\mathfrak{X}$ and $\bar{\mathfrak{X}}$ follow

$$\mathfrak{X} = \frac{c_a(22-c_a)}{5(1+2c_a)}, \tag{4.7}$$

$$\bar{\mathfrak{X}} = \frac{4c_a(1310+1679c_a+1629c_a^2-62c_a^3+7c_a^4)}{175(1+2c_a)^3}. \tag{4.8}$$

However, it is known that the Percus–Yevick equation does not give a good representation of the radial distribution function when the density of spheres is too high. On the basis of a comparison of Wertheim's solution (satisfying the Laplace transform (4.4) and hereafter denoted by the subscript W) with results obtained in numerical experiments, Verlet and Weis (1972) proposed an alternative and improved expression for the radial distribution function:

$$g(\rho;c_a) = g_W(\rho/\phi;\tilde{c}_a) + \delta g(\rho) \quad \text{for } \rho \geqslant 2. \tag{4.9}$$

First, in order to correct defects shown by $g_W(\rho;c_a)$ for large ρ, reduced radius $\tilde{a}$ (such that $\phi = \tilde{a}/a$) and volume concentration $\tilde{c}_a$ were introduced. These reduced parameters obey the relation

$$\tilde{a}^3 c_a = a^3 \tilde{c}_a, \tag{4.10}$$

with $\tilde{c}_a$ being given by the empirical formula:

$$\tilde{c}_a = c_a - \frac{1}{16}c_a^2. \tag{4.11}$$

Secondly, $\delta g(\rho)$ is a short-range term used to produce the correct behavior near the core ($\rho \sim 2$). This can be written as

$$\delta g(\rho) = \alpha\frac{\mathrm{e}^{-\beta(\rho-2)}}{\rho}\cos[\beta(\rho-2)], \tag{4.12}$$

with

$$\alpha = \frac{3}{2}\frac{\tilde{c}_a^2(1-0.7117\tilde{c}_a-0.114\tilde{c}_a^2)}{(1-\tilde{c}_a)^4} \quad \text{and} \quad \beta = 12\alpha\frac{(1-\tilde{c}_a)^2}{\tilde{c}_a(2+\tilde{c}_a)}. \tag{4.13}$$

The improved expression for the radial distribution function is now employed to derive $f(s)$ and the related $\mathfrak{X}$ and $\bar{\mathfrak{X}}$. Using definition (4.9), the integral in Eq. (4.3)

assumes the form

$$\int_0^\infty \rho g(\rho; c_a) e^{-s\rho}\, d\rho = \phi^2 \int_0^\infty \rho g_W(\rho; \tilde{c}_a) e^{-\phi s\rho}\, d\rho + \int_2^\infty \rho \delta g(\rho)\, e^{-s\rho}\, d\rho, \tag{4.14}$$

which can be easily evaluated by using Eqs. (4.4)–(4.5) and (4.12). Thus, one obtains:

$$f(s) = \frac{8\phi^3 s L(2\phi s; \tilde{c}_a)}{12\tilde{c}_a[L(2\phi s; \tilde{c}_a) + M(2\phi s; \tilde{c}_a) e^{2\phi s}]} + \alpha \frac{e^{-2s}(\beta + s)}{2\beta^2 + 2\beta s + s^2} - \frac{1}{s^2}. \tag{4.15}$$

Finally, introducing Eq. (4.15) into Eqs. (4.1)–(4.2) and taking the limits, $\mathfrak{X}$ and $\bar{\mathfrak{X}}$ can be derived for the improved statistical model:

$$\mathfrak{X} = \frac{\alpha + 4\beta}{2\beta} - \frac{\phi^2(10 - 2\tilde{c}_a + \tilde{c}_a^2)}{5(1 + 2\tilde{c}_a)}, \tag{4.16}$$

$$\bar{\mathfrak{X}} = \frac{8\beta^3 + 4\alpha\beta^2 - \alpha}{2\beta^3} - \frac{4\phi^4(175 - 260\tilde{c}_a + 421\tilde{c}_a^2 - 229\tilde{c}_a^3 + 62\tilde{c}_a^4 - 7\tilde{c}_a^5)}{175(1 + 2\tilde{c}_a)^3}, \tag{4.17}$$

with ϕ, $\tilde{c}_a$, α and β being functions of the effective volume fraction c_a according to Eqs. (4.10)–(4.11) and Eq. (4.13). To summarize, Eqs. (4.16) and (4.17) replace Eqs. (4.7) and (4.8) when the improved statistical model is employed.

It is important to mention that for very high volume fractions ($0.5 < c_a < 0.64$) the hard-sphere fluid system could adopt states characterized by some degrees of ordering (*fluid–solid phase transition*), that the Verlet–Weis radial distribution function cannot describe well (Torquato and Stell, 1985); such ordered states are not considered here. On the other hand, Høye and Stell (1976), and others, appear to find the Verlet–Weis approximation suitable for states characterized by no ordering (*glassy states*) even at very high densities ($0.5 < c_a < 0.64$). Unfortunately, the most recent studies on the functional behavior of the radial distribution function for dense systems of hard spheres have only focused on its contact value for $\rho = 2$ (Rintoul and Torquato, 1996).

5. Effects of inclusion shape on the nonlocal correction and exact results for matrices containing nonoverlapping identical spheres

In order to analyze the effects of inclusion/void shape on the nonlocal correction, this section deals with the derivation of the geometrical functions f_A, f_B and the related radial integrals appearing in expressions (3.23)–(3.24) of the nonlocal coefficients H, $\bar{H}$ for a specific inclusion/void shape that permits the nonlocal constitutive equation to be applied to a wide range of applications. Namely, nonoverlapping identical spheroids of semi-axes $a_1 = a_2 \neq a_3$ having random orientations are considered. The semi-major axis of the spheroids represents the characteristic semi-length $a = \max\{a_1, a_3\}$, whereas the shape is fixed by the aspect ratio $w = a_3/a_1$: $w < 1$ and $w > 1$ correspond to oblate

and prolate spheroids, respectively; of course, $w=1$ for the case of spheres. Note that the volume fractions of the spheroids and of their security spheres satisfy $c_1 = c_a w$ for oblate spheroids and $c_1 = c_a/w^2$ for prolate spheroids.

First, recall that function f_A is related to the intersection volume of two aligned inclusions/voids averaged over all possible orientations the inclusions/voids can take. As detailed in Appendix A, employing Eqs. (A.1)–(A.4) leads to the general definition of f_A in the case of spheroids

$$f_A(\rho) = \frac{w a_1^3}{2a^3} \int_0^\pi \left(1 - \frac{3}{4}\,\rho F(\theta) + \frac{1}{16}\,\rho^3 F(\theta)^3\right) \sin\theta \,\mathrm{d}\theta, \tag{5.1}$$

having defined here

$$F(\theta) = \frac{a}{w a_1} \sqrt{w^2 \sin^2\theta + \cos^2\theta}. \tag{5.2}$$

Notice that the angular integral in Eq. (5.1) can be easily evaluated in closed form for both oblate ($a_1{=}a, a_3{=}wa, w \leqslant 1$) and prolate ($a_1{=}a/w, a_3{=}a,\ w \geqslant 1$) spheroids. Then, using this result, integrals (3.25) can also be obtained analytically. Explicit expressions for the function f_A as well as for the integrals $\mathfrak{F}_A$, $\bar{\mathfrak{F}}_A$ can be found in Appendix A for both oblate and prolate spheroidal inclusions/voids.

Secondly, recall that function f_B is related to the intersection volume of two inhomogeneous spheres statistically equivalent to randomly oriented inclusions/voids. Let S denote a spherical shell of radius r, concentric with the reference inclusion/void. Varying r from 0 to a, the statistical density γ of the equivalent inhomogeneous sphere is defined as the ratio between the portion of S falling into the particle and the total surface of S. In the case under consideration, for $r \leqslant c$ ($c = \min\{a_1, a_3\}$ being the semi-minor axis of the spheroids) S falls entirely into the reference spheroid, then $\gamma = 1$. For $c < r \leqslant a$, two spherical caps of height $\tilde{h} = r - \sqrt{(a_3^2 - r^2 w^2)/(1-w^2)}$ arranged symmetrically about the plane $a_1,\ a_2$ are obtained from the intersection of S with the reference spheroid; such two spherical caps represent the portion of S falling into/out of the prolate/oblate spheroid with surface area $4\pi r\tilde{h}$ as a function of r which depends also on the prolate/oblate spheroidal shape through the aspect ratio. It follows that

$$\gamma(\rho) = \begin{cases} 1, & 0 \leqslant \rho \leqslant c/a, \\ f(\rho), & c/a < \rho \leqslant 1, \end{cases} \tag{5.3}$$

where it is straightforward to show that

$$f(\rho) = \begin{cases} \dfrac{w}{\rho}\sqrt{\dfrac{1-\rho^2}{1-w^2}} & \text{for } w < 1 \ (c = wa), \\[2ex] 1 - \dfrac{1}{\rho}\sqrt{\dfrac{w^2\rho^2 - 1}{w^2 - 1}} & \text{for } w > 1 \ (c = a/w). \end{cases} \tag{5.4}$$

Then, the intersection volume of two such inhomogeneous spheres can be evaluated following the approach detailed in Appendix B and setting $b = \bar{b} = a$ and $f = \bar{f} = \gamma$.

From Eqs. (B.4) to (B.6), the general definition for f_B can be obtained

$$f_B(\delta) = \frac{3}{2}\begin{cases} \displaystyle\int_0^{1-\delta} \rho^2\gamma(\rho)\left(\int_0^{\pi}\gamma(\bar{\rho})\sin(\phi)\,\mathrm{d}\phi\right)\mathrm{d}\rho & 0 \leqslant \delta < 1, \\ \quad\displaystyle+\int_{1-\delta}^{1}\rho^2\gamma(\rho)\left(\int_0^{\bar{\phi}}\gamma(\bar{\rho})\sin(\phi)\,\mathrm{d}\phi\right)\mathrm{d}\rho & \\ \displaystyle\int_{\delta-1}^{1}\rho^2\gamma(\rho)\left(\int_0^{\bar{\phi}}\gamma(\bar{\rho})\sin(\phi)\,\mathrm{d}\phi\right)\mathrm{d}\rho & 1 \leqslant \delta < 2, \end{cases} \tag{5.5}$$

having defined

$$\bar{\rho} = \sqrt{\rho^2 - 2\delta\rho\cos\phi + \delta^2} \quad \text{and} \quad \bar{\phi} = \arccos\left(\frac{\rho^2+\delta^2-1}{2\delta\rho}\right). \tag{5.6}$$

It is obvious that the integrals in Eq. (5.5) may be either difficult or impossible to obtain analytically for arbitrary oblate/prolate spheroidal shape because of the complexity of $\gamma(\rho)$. It follows that, except for some special cases, f_B and its related radial integrals in expressions (3.23) and (3.24) of H and $\bar{H}$ are not known explicitly. However, approximate but analytical results for different cases of spheroid shape can be obtained, as discussed in Section 6.

The case of nonoverlapping identical spheres of radius a as special case of spheroids with aspect ratio $w = 1$ ($c_a = c_1$) is now analyzed. This particular shape permits the analytical evaluation of all the shape-dependent integrals and the attainment of exact results for the nonlocal coefficients H and $\bar{H}$.

First, taking the correct directional limit of (A.10)–(A.13) for $w \to 1$ provides $\mathfrak{F}_A$ and $\bar{\mathfrak{F}}_A$ that reduce to constants:

$$\mathfrak{F}_A = \tfrac{2}{5} \quad \text{and} \quad \bar{\mathfrak{F}}_A = \tfrac{12}{35}. \tag{5.7}$$

Secondly, notice that in this particular case $f_B = f_A$ is the well-known intersection function of two identical spheres (see, e.g., Markov and Willis, 1998):

$$f_B(\delta) = 1 - \tfrac{3}{4}\,\delta + \tfrac{1}{16}\,\delta^3 \quad \text{for } 0 \leqslant \delta \leqslant 2. \tag{5.8}$$

Using this result, all radial integrals in Eqs. (3.23) and (3.24) can be easily evaluated, so that in the case of spheres, H and $\bar{H}$ assume the forms

$$H = \frac{a^2}{5(1-c_1)}\,[2 + c_1(-9 + 5\mathfrak{X})], \tag{5.9}$$

$$\bar{H} = \frac{a^4}{175(1-c_1)}[60 + c_1(-834 + 70\mathfrak{X} + 175\bar{\mathfrak{X}})], \tag{5.10}$$

where $\mathfrak{X}$ and $\bar{\mathfrak{X}}$ have been derived in closed form in Section 4 for two different statistical models for the radial distribution function.

Verification for Eqs. (5.9) and (5.10) can be found in Drugan and Willis (1996) and Drugan (2000) who derived completely explicit results using the Percus–Yevick

model. Their results can be reproduced by substituting expressions (4.7) and (4.8) for $\mathfrak{X}$ and $\bar{\mathfrak{X}}$ in Eqs. (5.9) and (5.10), so that we obtain:

$$H = a^2 \frac{(2-c_1)(1-c_1)}{5(1+2c_1)}, \tag{5.11}$$

$$\bar{H} = \frac{2}{175} a^4 \frac{(1-c_1)(30-177c_1+248c_1^2-124c_1^3+14c_1^4)}{(1+2c_1)^3}. \tag{5.12}$$

Alternatively, improved results based on an improved choice of the statistical model, namely the Verlet–Weis correction to the Percus–Yevick model, can be derived. In order to do this, Eqs. (5.9) and (5.10) must be combined with expressions (4.16) and (4.17) for $\mathfrak{X}$ and $\bar{\mathfrak{X}}$, so that for the improved statistical model we finally have

$$H = a^2 \frac{5\alpha c_1(1+2\tilde{c}_1)+2\beta[(1+2\tilde{c}_1)(2+c_1)-c_1\phi^2(10-2\tilde{c}_1+\tilde{c}_1^2)]}{10\beta(1-c_1)(1+2\tilde{c}_1)}, \tag{5.13}$$

$$\bar{H} = \frac{2a^4}{175(1-c_1)}\left\{3(10+c_1) - \frac{35\alpha c_1(5-22\beta^2)}{4\beta^3} - \frac{7\phi^2 c_1(10-2\tilde{c}_1+\tilde{c}_1^2)}{(1+2\tilde{c}_1)} - \frac{2\phi^4 c_1(175-260\tilde{c}_1+421\tilde{c}_1^2-229\tilde{c}_1^3+62\tilde{c}_1^4-7\tilde{c}_1^5)}{(1+2\tilde{c}_1)^3}\right\}, \tag{5.14}$$

where ϕ, $\tilde{c}_1$, α and β are functions of the effective volume fraction $c_a = c_1$ according to Eqs. (4.10)–(4.11) and (4.13). Thus, Eqs. (5.13) and (5.14) can be used to replace Eqs. (5.11) and (5.12) in the derivation of a completely explicit nonlocal constitutive equation for an isotropic matrix reinforced/weakened by a random and isotropic distribution of isotropic spherical inclusions/voids. As an application, in Section 7.1 the nonlocal constitutive equation so specialized is employed to compare estimates of minimum RVE size as functions of volume fraction for these two different choices of the statistical model.

6. Approximate closed-form solutions for matrices containing randomly oriented spheroids

The use of nonspherical particles requires a more elaborate evaluation of the shape-dependent integrals involved in expressions (3.23) and (3.24) of H and $\bar{H}$ as compared to the case of spheres analyzed in the previous section. The derivation of function f_B itself, as the intersection function of two identical inhomogeneous spheres statistically equivalent to randomly oriented spheroids, may be difficult since additional integrals of the statistical density function γ are involved. It follows that only approximate closed-form results can be produced. To facilitate these, particular shapes of particles are considered. This permits one to assume simplified representations for the statistical density function, so that the shape-dependent integrals mentioned above can be

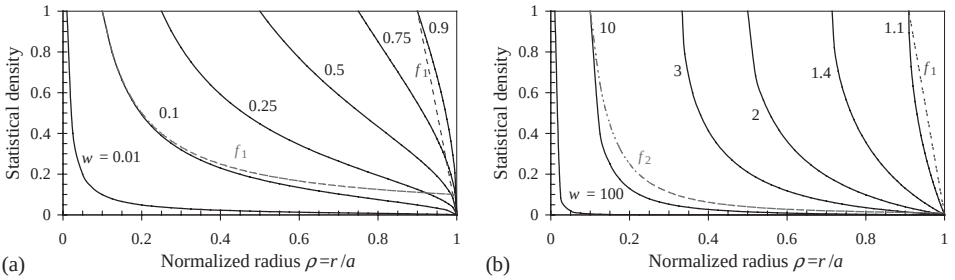

Fig. 2. Statistical density function for (a) oblate and (b) prolate spheroids.

expressed approximately but in closed form. These integrals have also been evaluated numerically for a wide range of spheroid aspect ratios (see Section 7.3).

Now, recall that, according to the model of impenetrable particles introduced in Section 3, each randomly oriented spheroid is thought of as being replaced by a statistically equivalent inhomogeneous sphere with density varying radially outside a homogeneous core of radius c, the semi-minor axis of the spheroid. The related statistical density function, already given by Eqs. (5.3) and (5.4), is shown in Fig. 2 (solid lines) for both oblate ($w = 0.01$, 0.1, 0.25, 0.5, 0.75, 0.9) and prolate ($w = 1.1$, 1.4, 2, 3, 10, 100) spheroids of varying aspect ratio. One can observe that quite different trends characterize the statistical densities of oblate (Fig. 2a) and prolate (Fig. 2b) spheroids. However, in the limits $c \to 0$ (disk/needle-shaped particles) and $c \to a$ (nearly spherical particles) good approximations can be sought in the same families of functions, as detailed in this section.

Since the discussion is entirely based on approximating the function $\gamma(r)$ by another function $\hat{\gamma}(r)$ on $[0,a]$, a convenient measure of approximation must be defined to quantify how close γ and $\hat{\gamma}$ are. This is not only important to define the accuracy of the approximation, but the related restrictions on the class of materials for which the model can still provide accurate results. To assess the approximation accuracy in an average sense, the root-mean-square error E is often used (Atkinson, 1989), where

$$E = \frac{1}{\sqrt{a}} \sqrt{\int_0^a [\gamma(r) - \hat{\gamma}(r)]^2 \, \mathrm{d}r}, \tag{6.1}$$

and $E \times 100$ is defined as the percentage error of the approximation. According to Eq. (5.3), we assume $\hat{\gamma}(r) = 1$ on $[0,c]$ and $\hat{\gamma}(r) = \hat{f}(r)$ on $[c,a]$, $\hat{f}(r)$ being the approximation of $f(r)$. Thus, Eq. (6.1) simplifies to:

$$E = \frac{1}{\sqrt{a}} \sqrt{\int_0^a [\gamma(r) - \hat{\gamma}(r)]^2 \, \mathrm{d}r} = \frac{1}{\sqrt{a}} \sqrt{\int_c^a [f(r) - \hat{f}(r)]^2 \, \mathrm{d}r}$$

$$= \sqrt{\int_{c/a}^1 [f(\rho) - \hat{f}(\rho)]^2 \, \mathrm{d}\rho}. \tag{6.2}$$

6.1. Nearly spherical inclusions/voids

This case can be regarded as special case of oblate/prolate spheroids with aspect ratio $w \lesssim 1/w \gtrsim 1$. For such aspect ratios tending to unity, the approximation of function f may be sought in the following family $\mathscr{F}$ of functions

$$f_n(\rho) = \frac{1-\rho^n}{1-(c/a)^n}, \quad n > 0, \tag{6.3}$$

which satisfy both conditions: $f_n(c/a) = 1$ and $f_n(1) = 0$. To find n, a least-square approximation problem may be solved. On the other hand, it is straightforward to show that $n = 1$ gives a sufficiently good approximation (i.e. $< 6\%$ error) for both oblate and prolate spheroids, provided w is in the range [0.8, 1.1]. Then, we may assume:

$$\hat{f}(\rho) = f_1(\rho) = \begin{cases} \dfrac{1-\rho}{1-w} & \text{for } w \lesssim 1 (c/a = w), \\ w\,\dfrac{1-\rho}{w-1} & \text{for } w \gtrsim 1 (c/a = 1/w). \end{cases} \tag{6.4}$$

Fig. 2 shows the approximation function f_1, e.g., for $w = 0.9$, 1.1 (dotted lines). Note that in the case of oblate spheroids only slightly more accurate approximations ($\leqslant 5\%$ against $< 6\%$ error) could be obtained by taking $n > 1$. On the contrary, for prolate spheroids f_1 always represents the best approximation of f, that is the closest function to f in $\mathscr{F}$. Of course, the greater the aspect ratio, the less accurate the approximation (e.g., 9% error for $w = 1.2$).

Approximation (6.4) is now used to evaluate all radial integrals in Eqs. (3.23) and (3.24). First, the intersection function f_B is obtained by following the approach suggested in Appendix B. Then, the result is used to evaluate the additional radial integrals. Finally, substituting into Eqs. (3.23) and (3.24) leads to H and $\bar{H}$. Thus, in the case of nearly spherical inclusions/voids one obtains

$$H = \frac{c_a a^2}{c_1(1-c_1)} \left\{ \mathfrak{F}_A + \frac{c_a}{240} [2\omega_1 (1+w)^2 (1+w^2) + 15 \mathfrak{X} \omega_2 (1+w+w^2+w^3)^2] \right\}, \tag{6.5}$$

$$\bar{H} = \frac{c_a a^4}{c_1(1-c_1)} \left\{ \bar{\mathfrak{F}}_A + \frac{c_a}{240 \times 420} (1+w)^2 [\omega_3 + 1680 \mathfrak{X} \omega_4 (1+2w^2+2w^4+w^6)] + \frac{c_a}{16} \bar{\mathfrak{X}}\, \omega_2 (1+w+w^2+w^3)^2 \right\}, \tag{6.6}$$

where for oblate spheroids

$$\begin{aligned} &\omega_1 = -14 - 14w^2 + w^4, \quad \omega_2 = 1, \quad \omega_4 = 1 \\ &\omega_3 = -28459 - 56918\ w^2 - 31662\ w^4 - 3158\ w^6 + 101\ w^8 \end{aligned} \quad \text{for } w \lesssim 1, \tag{6.7}$$

whereas for prolate spheroids

$$\omega_1 = \frac{1 - 14w^2 - 14w^4}{w^8}, \quad \omega_2 = \frac{1}{w^6}, \quad \omega_4 = \frac{1}{w^8}$$
$$\omega_3 = \frac{101 - 3158w^2 - 31662w^4 - 28459w^6(2 + w^2)}{w^{10}} \quad \text{for } w \gtrsim 1. \tag{6.8}$$

In Eqs. (6.5) and (6.6) $\mathfrak{F}_A$ and $\bar{\mathfrak{F}}_A$ are still given by Eqs. (A.10)–(A.13), while $\mathfrak{X}$ and $\bar{\mathfrak{X}}$ are expressed by either Eqs. (4.7)–(4.8) or Eqs. (4.16)–(4.17) depending on the choice of either the standard or the improved statistical model. Once again, just as final confirmation, notice that in the limit $w \to 1$ Eqs. (6.5) and (6.6) reduce precisely to the exact results (5.9) and (5.10) shown for spheres.

An application of these results is provided in Section 7.2, where the nonlocal constitutive equation is employed to analyze shape effects on minimum RVE size, for the case of an isotropic matrix reinforced/weakened by a random and isotropic distribution of isotropic nearly spherical inclusions/voids randomly oriented. As a complementary check and extension of these approximate analytical results, estimates of minimum RVE size based on highly accurate numerical evaluations of the shape-dependent integrals, for a wide range of spheroid aspect ratios, are provided in Section 7.3.

6.2. Disk/needle-shaped inclusions/voids

The case of disks and needles can be regarded as special case of spheroids with semi-minor axis $c \to 0$. Oblate spheroids ($c = wa$) with aspect ratio $w \to 0$ represent disks, while needles can be thought of as prolate spheroids ($c = a/w$) with $w \gg 1$. In both cases, the approximation of statistical density function f may be sought in the following family F of functions

$$f_n(\rho) = \frac{(c/a)^n}{\rho^n}, \quad n > 0, \tag{6.9}$$

which satisfy only the condition: $f_n(c/a) = 1$, whereas $f_n(1)$ vanishes like $(c/a)^n$ for c tending to zero and so very quickly for both very small and very big aspect ratios. The exponent n is taken so that the related root-mean-square error E is minimized. In the case of oblate spheroids it is straightforward to show that, for small w, $n = 1$ gives the best approximation for f in $\mathfrak{F}$. The related error is $\leqslant 7\%$ for $w < 0.2$, which decreases to $< 4\%$ for $w \leqslant 0.1$. On the contrary, in the case of prolate spheroids the same level of accuracy can be attained only by taking at least $n = 2$. This corresponds to a sufficiently good approximation (i.e. $< 7\%$ error) for $w \geqslant 10$, which becomes more accurate (i.e. $< 5\%$ error) for $w \geqslant 20$. In Fig. 2 the functions f_1 (dashed lines) and f_2 (dot-dashed lines) are shown, e.g., for $w = 0.1$ and for $w = 10$, respectively. To summarize, the following approximations for the density function $f(\rho)$ may be

assumed

$$\hat{f}(\rho) = \begin{cases} f_1(\rho) = \dfrac{w}{\rho} & \text{for } w < 0.2, \\ f_2(\rho) = \dfrac{1}{w^2\rho^2} & \text{for } w \geqslant 10. \end{cases} \tag{6.10}$$

As already described for nearly spherical inclusions/voids, first Eq. (6.10) is used to obtain the intersection function f_B. To do this, since in the case under consideration the homogeneous cores of radius c almost disappear for both $w \ll 1$ and $w \gg 1$, their contributions to f_B can be neglected. Then, the result so obtained is integrated radially according to Eqs. (3.23) and (3.24) and thus H and $\bar{H}$ are derived. Notice that the simplified approach followed permits one to evaluate the leading-order of the radial integrals in w, that is w^2/w^{-4} for oblate/prolate spheroids. It follows that in the limits $w \to 0$ and $w \to \infty$ both H and $\bar{H}$ vanish like w and w^{-2}, respectively. As a consequence, perhaps surprisingly, the nonlocal coefficients also vanish. On the other hand, this result finds justification in the standard Hashin–Shtrikman variational formulation itself if applied to the limiting cases of cracks, disks and needles. As already outlined in the framework of local theories, more sophisticated approaches must be followed in these cases (see, e.g., Ponte Castañeda and Willis, 1995).

7. Quantitative estimates for minimum size of material volume elements

Standard approaches to modeling constitutive behavior of elastic composite materials develop local constitutive equations relating mean or ensemble averages of stress and strain fields through a constant effective modulus tensor. A tacit assumption of these models is that material volume elements are much larger than the microscopic scale of the material. A crucial issue for accurate application of such models is to derive quantitative estimates of the minimum size of a material volume element over which a constitutive model of this form is expected to provide a sensible description of the constitutive response of the composite.

That was one principal objective of Drugan and Willis (1996), who analysed the accuracy of a local constitutive equation of the form:

$$\langle\sigma\rangle_{ij}(\mathbf{x}) = \hat{L}_{ijkl}\langle e\rangle_{kl}(\mathbf{x}), \tag{7.1}$$

with respect to a nonlocal constitutive description of the form given by Eq. (2.1) where only the first nonlocal term was retained. In order to do this, ensemble-averaged strain fields sinusoidally varying with position were considered and the wavelength of the variation at which the nonlocal correction to the local term in the constitutive equation is not negligible was determined. In particular, quantitative results were obtained for two-phase composites consisting of an isotropic matrix reinforced/weakened by a random and isotropic distribution of nonoverlapping isotropic spherical particles/voids. More recently, Drugan (2000) used the higher-order form of the nonlocal constitutive equation (2.1) and provided more accurate estimates of minimum RVE size for the same type of composite. This permitted refinement but largely confirmation of Drugan and Willis' results characterized by surprisingly small RVE sizes even for high volume

concentrations of inclusions. In both analyses, the statistical model for the dispersion of nonoverlapping spheres incorporates up through two-point correlation functions and is based on the analytical solution, due to Wertheim (1963), of the Percus–Yevick equation for the radial distribution function. The Percus and Yevick (1958) model is the best-known statistical mechanics model for the radial distribution function; nevertheless, Wertheim's exact solution in the case of hard spheres has been shown to give an imperfect representation for high sphere densities.

Here, two new sets of results are described. First, previous quantitative estimates of minimum RVE size for the case of spherical inclusions/voids are re-examined by using a more accurate expression of the radial distribution function, as proposed by Verlet and Weis (1972) on the basis of a semi-empirical approach. Second, in order to analyze how the shape of inclusions affects the minimum RVE size, matrices containing randomly oriented spheroidal particles/voids are considered; namely, approximate analytical estimates are provided for nearly spherical inclusions/voids, and accurate numerical estimates are given for spheroidal voids having a wide range of aspect ratios.

The same simple case examined by both Drugan and Willis (1996) and Drugan (2000) is employed. An ensemble-averaged normal strain sinusoidally varying with position in its direction of straining is assumed

$$\langle e\rangle_{11}(\mathbf{x}) = e\sin\frac{2\pi x_1}{l}, \quad \langle e\rangle_{ij}(\mathbf{x}) = 0 \ \ \forall i,j \ \text{ except for } \ i=j=1, \tag{7.2}$$

where $|e| \ll 1$ is a pure number. Using Eq. (2.1), the related 11-component of ensemble average stress is

$$\begin{aligned}\langle\sigma\rangle_{11}(\mathbf{x}) &= \hat{L}_{1111}\langle e\rangle_{11}(\mathbf{x}) + \hat{L}^{(1)}_{111111}\frac{\partial^2\langle e\rangle_{11}(\mathbf{x})}{\partial x_1^2} + \hat{L}^{(2)}_{11111111}\frac{\partial^4\langle e\rangle_{11}(\mathbf{x})}{\partial x_1^4}\\ &= \left[\hat{L}_{1111} - \frac{4\pi^2}{l^2}\hat{L}^{(1)}_{111111} + \frac{16\pi^4}{l^4}\hat{L}^{(2)}_{11111111}\right] e\sin\frac{2\pi x_1}{l}.\end{aligned} \tag{7.3}$$

Defining $\varepsilon \times 100$ as the percentage correction provided by nonlocal terms to the constant effective modulus term, Drugan (2000) obtained the following equation for the minimum RVE size l:

$$\left|-\frac{4\pi^2}{l^2}\hat{L}^{(1)}_{111111} + \frac{16\pi^4}{l^4}\hat{L}^{(2)}_{11111111}\right| = \varepsilon|\hat{L}_{1111}|, \tag{7.4}$$

which reduces to that derived by Drugan and Willis (1996), if the second nonlocal term is set to zero:

$$\left|-\frac{4\pi^2}{l^2}\hat{L}^{(1)}_{111111}\right| = \varepsilon\left|\hat{L}_{1111}\right|. \tag{7.5}$$

In particular, the two extreme cases of a matrix weakened by voids ($\kappa_1 = \mu_1 = 0$) and a matrix reinforced by rigid particles ($\kappa_1 = \mu_1 = \infty$) are considered. Recalling that the elastic moduli for an isotropic material are related as $\kappa = [2\mu(1+\nu)/3(1-2\nu)]$ with ν the Poisson ratio, estimates so obtained turn out to be dependent only on the matrix

Poisson ratio. In particular, two classes of matrix materials $v \approx 0.2$ (e.g., glass, alumina, concrete) and $v \approx 0.33$ (e.g., aluminum, steels, copper, titanium) are considered for both types of "reinforcement".

7.1. Spherical inclusions/voids

According to the improved statistical model, Eqs. (5.13) and (5.14) have been used to evaluate local and nonlocal tensor components through Eqs. (2.2)–(2.14); then, Eqs. (7.4) and (7.5) have been employed to derive quantitative estimates of minimum RVE size. The minimum RVE size (normalized by the reinforcement diameter $2a$) computed for 5% error is displayed in boldface in Tables 1 and 2. These estimates are compared with Drugan and Willis' and Drugan's predictions obtained by using the standard Percus–Yevick–Wertheim form for the radial distribution function. Recall that this second set of results has been derived by using Eqs. (5.11) and (5.12) to evaluate nonlocal coefficients in Eqs. (7.4) and (7.5).

The results shown permit several interesting conclusions, in general confirming at lower sphere volume fractions ($c_1 < 0.25$) but correcting at higher ones, the previous Drugan and Willis (1996) and Drugan (2000) estimates. Overall, using the standard Wertheim form for the radial distribution function leads to underestimates of the minimum RVE sizes, by up to a factor greater than two at high inclusion and void concentrations. Recall that in the Percus–Yevick–Wertheim case, even for quite good accuracy (i.e. 5% error) and using the higher-order nonlocal constitutive equation, the minimum RVE size first increases with increasing particle volume fraction until a maximum is attained at 0.25–0.35 volume fraction (denoted in italics in tables) depending on the reinforcement type; then, it starts to decrease slightly. At the maximum a remarkably small minimum RVE size of approximately two reinforcement diameters is found for any class of structural materials (matrix Poisson's ratios 0.2 and 0.33) and reinforcement type (including the extreme cases of spherical voids and rigid particles analyzed here). On the contrary, improved minimum RVE sizes calculated using the Verlet–Weis model increase monotonically with increasing particle volume concentration. Close to the maximum packing density (0.64 volume fraction) quite good accuracy for validity of local constitutive equation (7.1) is restricted to material volume elements having sizes of at least approximately 4.5–5 particle diameters for all matrix materials and reinforcement types considered. For higher accuracy (1% error), the RVE size required exceeds about 10 times the reinforcement diameter. Also, voids are confirmed to have longer-range effects than rigid particles. In fact, the minimum RVE size required for the same accuracy of the local constitutive model is always larger for the matrix weakened by voids than for that reinforced by rigid particles.

7.2. Approximate analytical results for nearly spherical inclusions/voids

This new set of results has been obtained by using the lower-order equation (7.5) for the minimum RVE size. Furthermore, on the basis of previous conclusions, the improved Verlet–Weis statistical model for the radial distribution function of security spheres has been assumed. Thus, Eqs. (4.16) and (4.17) have been used to evaluate

Table 1
Comparison of minimum RVE sizes for matrices weakened by spherical voids based on two different choices of the radial distribution function: standard Wertheim form and improved Verlet–Weis form (in bold)

c_1	Minimum RVE size $l/(2a)$ for spherical voids, for 5% error			
	$\nu = 0.2$		$\nu = 0.33$	
	Based on one nonlocal term—Eq. (6.5)	Based on two nonlocal terms—Eq. (6.4)	Based on one nonlocal term—Eq. (6.5)	Based on two nonlocal terms—Eq. (6.4)
0.025	1.005	1.177	1.018	1.232
	1.005	**1.178**	**1.019**	**1.232**
0.05	1.345	1.490	1.363	1.539
	1.346	**1.491**	**1.363**	**1.540**
0.10	1.710	1.825	1.729	1.863
	1.715	**1.828**	**1.734**	**1.867**
0.15	1.887	1.985	1.906	2.015
	1.903	**1.993**	**1.922**	**2.024**
0.20	1.967	2.052	1.984	2.077
	2.007	**2.070**	**2.025**	**2.097**
0.25	*1.987*	*2.063*	*2.003*	*2.083*
	2.073	**2.097**	**2.089**	**2.120**
0.30	1.968	2.035	1.981	2.052
	2.137	**2.095**	**2.151**	**2.117**
0.35	1.921	1.982	1.933	1.995
	2.233	**2.079**	**2.247**	**2.104**
0.40	1.854	1.909	1.864	1.920
	2.404	**2.066**	**2.417**	**2.101**
0.45	1.772	1.822	1.781	1.831
	2.697	**2.125**	**2.710**	**2.184**
0.50	1.679	1.725	1.686	1.732
	3.168	**2.575**	**3.181**	**2.621**
0.55	1.577	1.619	1.583	1.624
	3.884	**3.419**	**3.898**	**3.448**
0.60	1.467	1.506	1.472	1.510
	4.934	**4.592**	**4.948**	**4.614**

Results computed for 5% error in validity of Eq. (7.1).

local and nonlocal coefficients in Eq. (7.5) through Eqs. (2.2)–(2.14) together with Eqs. (6.5)–(6.8). With reference to an isotropic matrix having $\nu = 0.33$, Figs. 3 and 4 show the minimum RVE size (normalized by the spheroid major axis $2a$) computed for 5% error by varying the aspect ratio of spheroids. These estimates are compared with previous predictions obtained for spherical inclusions (dotted lines). Recall that, because of the simplifying assumption of randomly oriented spheroids placed within hard "security" spheres, the analysis has been restricted up to the maximum packing density for nonoverlapping spheres ($c_a = 0.64$), which corresponds to lower maximum volume fractions for spheroids depending on their aspect ratio.

Analogously to the previous set of results described in Section 7.1, the type of "reinforcement" appears to play a secondary role. Once again, the minimum RVE size

Table 2
Comparison of minimum RVE sizes for matrices reinforced by spherical rigid particles based on two different choices of the radial distribution function: standard Wertheim form and improved Verlet–Weis form (in bold)

c_1	Minimum RVE size $l/(2a)$ for spherical rigid particles, for 5% error			
	$\nu = 0.2$		$\nu = 0.33$	
	Based on one nonlocal term—Eq. (6.5)	Based on two nonlocal terms—Eq. (6.4)	Based on one nonlocal term—Eq. (6.5)	Based on two nonlocal terms—Eq. (6.4)
0.025	1.005	0.9449	0.8513	0.8821
	1.005	**0.9447**	**0.8514**	**0.8819**
0.05	1.345	0.9796	1.144	0.9218
	1.346	**0.9802**	**1.144**	**0.9224**
0.10	1.710	0.9323	1.462	0.8838
	1.715	**0.9391**	**1.467**	**0.8905**
0.15	1.887	1.422	1.623	0.8092
	1.903	**0.8770**	**1.637**	**0.8347**
0.20	1.967	1.728	1.701	1.402
	2.007	**1.695**	**1.736**	**0.8001**
0.25	*1.987*	1.821	*1.727*	1.540
	2.073	**1.778**	**1.801**	**1.355**
0.30	1.968	*1.844*	1.718	1.584
	2.137	**1.757**	**1.865**	**0.8909**
0.35	1.921	1.826	1.684	*1.585*
	2.233	**1.052**	**1.958**	**1.027**
0.40	1.854	1.780	1.632	1.556
	2.404	**1.228**	**2.116**	**1.203**
0.45	1.772	1.714	1.566	1.508
	2.697	**1.424**	**2.383**	**1.397**
0.50	1.679	1.634	1.489	1.445
	3.168	**1.627**	**2.809**	**1.599**
0.55	1.577	1.542	1.403	1.370
	3.884	**1.837**	**3.455**	**1.807**
0.60	1.467	1.441	1.309	1.286
	4.934	**4.151**	**4.402**	**2.035**

Results computed for 5% error in validity of Eq. (7.1).

is always larger for the matrix weakened by voids (Fig. 4) than for that reinforced by rigid particles (Fig. 3), but the same conclusions can be drawn in both cases. On the contrary, the shape of spheroids appears to affect considerably the nonlocal correction, as outlined below.

Overall, minimum RVE sizes increase monotonically with increasing volume concentration of spheroids and the same trend as for spheres is shown. In general, oblate spheroids (dashed lines) have longer-range effects than prolate spheroids (solid lines). More interestingly, at lower densities the minimum RVE size required for the same accuracy (5% error) of the local constitutive model is always larger for the matrix containing spheres than for that embedding spheroids of whatever aspect ratio, whereas

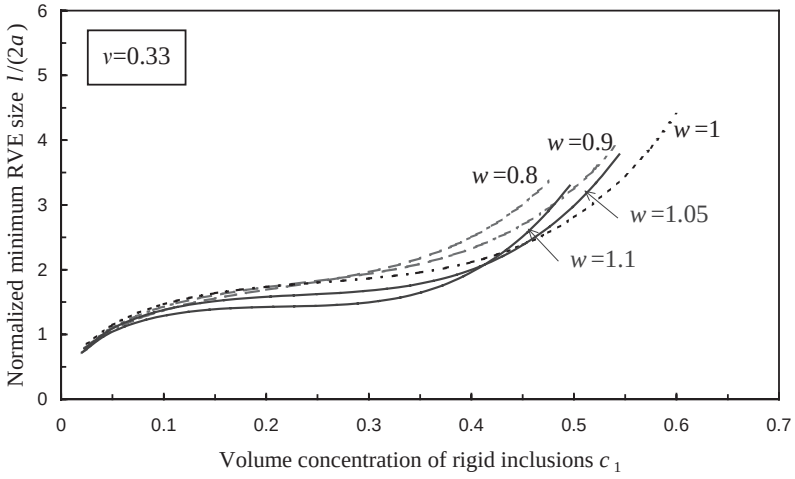

Fig. 3. Minimum RVE size for matrices reinforced by rigid spheroids, computed for $v = 0.33$ and 5% error in validity of Eq. (7.1).

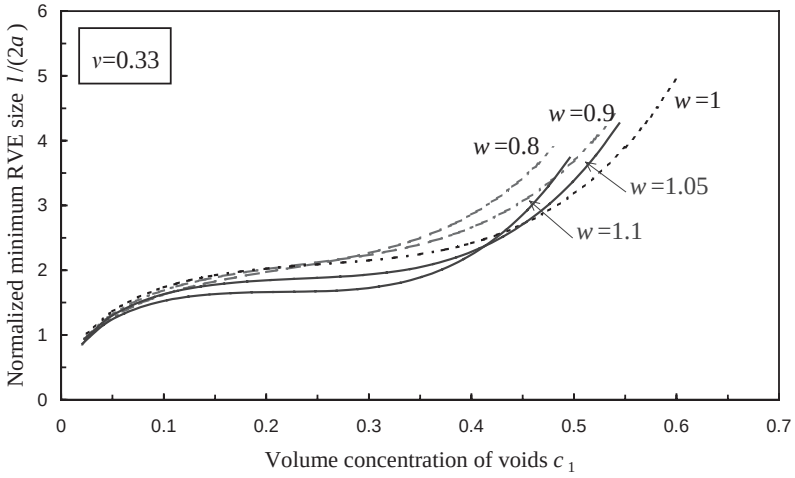

Fig. 4. Minimum RVE size for matrices weakened by spheroidal voids, computed for $v = 0.33$ and 5% error in validity of Eq. (7.1).

at higher densities spheroids have stronger interaction effects than spheres. The critical value of density at which spheres and spheroidal particles induce the same nonlocal correction depends on the shape of spheroids and is larger for prolate (about $c_1 = 0.42$) than for oblate (about $c_1 = 0.25$) ones.

In conclusion, at low volume fractions, results obtained in the case of spheres slightly overestimate effective RVE sizes for matrices weakened/reinforced by spheroidal

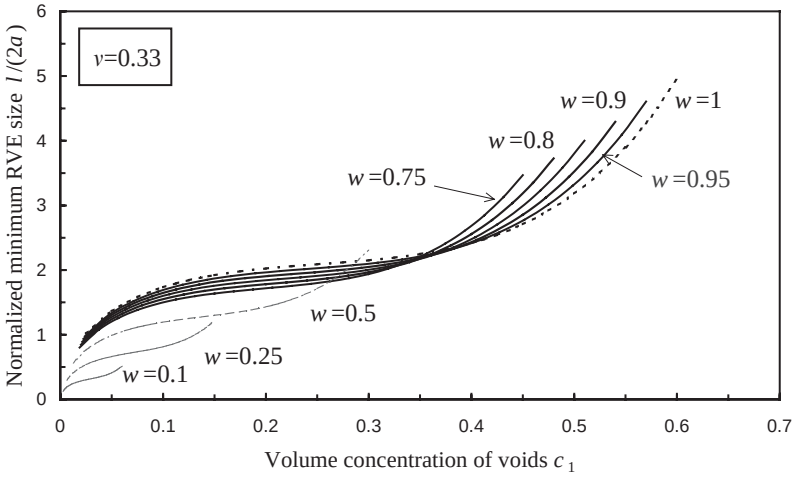

Fig. 5. Minimum RVE size for matrices weakened by oblate spheroidal voids, computed for $\nu = 0.33$ and 5% error in validity of Eq. (7.1).

voids/inclusions having major axis equal to the sphere diameter. At high volume fractions, the more the aspect ratio of spheroidal heterogeneities differs from unity, the larger the material volume element required for good accuracy of the local constitutive equation (7.1). As an example, for quite good accuracy (i.e., 5% error), close to $c_1 = 0.5$ the normalized minimum RVE size is about 3 in the case of spheres, 3.5 for $w = 0.8$ and 4 for $w = 1.1$.

7.3. Numerical results for spheroidal voids

As a check on, and extension of, the approximate analytical results of Section 7.2, another set of results has been obtained by evaluating numerically the nonlocal coefficients (3.23) and (3.24) for specific values of w, for a wider range of w values than was possible in the approximate analytical approach. This has involved exact analytical evaluation of the ϕ-integral in function f_B of Eq. (5.5) and numerical evaluation of the remaining double integral (that is, simultaneously, the ρ-integral in f_B and the radial integrals of f_B in Eqs. (3.23) and (3.24)). Figs. 5 and 6 show quantitative RVE estimates computed for $\nu = 0.33$ matrices weakened by spheroidal voids of aspect ratios $w = 0.1$, 0.25, 0.5, 0.75, 0.8, 0.85, 0.9, 0.95 (oblate spheroids) and $w = 1.025$, 1.05, 1.1, 1.2, 1.4, 2, 3 (prolate spheroids). Results are presented only for the case of voids, which as noted earlier always lead to larger minimum RVE sizes than do rigid inclusions.

The numerical results in general confirm the analytical estimates of minimum RVE size shown in Fig. 4 and derived in Section 7.2 on the basis of approximating the density function γ in Eq. (5.5) to permit analytical evaluation of all integrals mentioned above. In particular, the highly accurate numerical results presented here confirm all

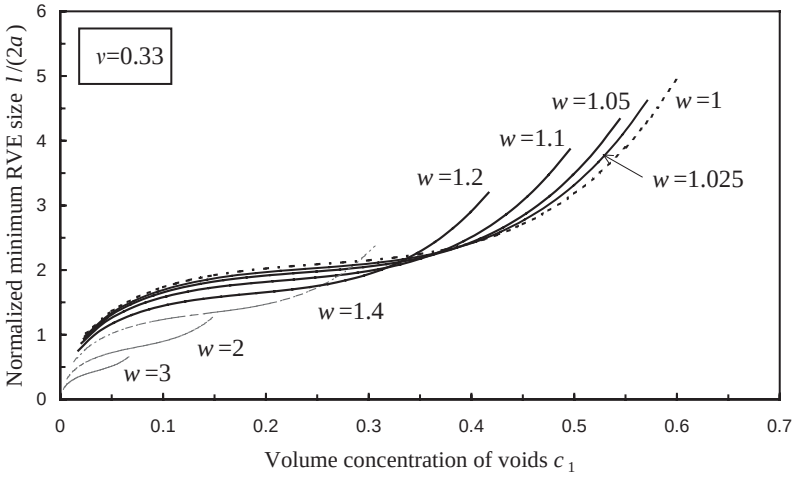

Fig. 6. Minimum RVE size for matrices weakened by prolate spheroidal voids, computed for $\nu = 0.33$ and 5% error in validity of Eq. (7.1).

of the features of the results described in Section 7.2. As for quantitative comparisons, for oblate spheroids, approximation of function γ in Section 7.2 has lead to (analytical) overestimates of minimum RVE size, the percentage error ranging from about 1% for $w=0.99$ to about 15% for $w=0.8$ (5% for $w=0.95$, 10% for $w=0.9$, 13% for $w=0.85$). For prolate spheroids, the use of an approximated density function in Section 7.2 has lead to (analytical) underestimates of minimum RVE size; the percentage error ranges from about 1% for $w = 1.01$ to about 13% for $w = 1.1$ (3% for $w = 1.025$, 6% for $w = 1.05$) depending on the prolate spheroid aspect ratio.

Finally, the smaller/larger the aspect ratio, the smaller the minimum RVE required for good accuracy of the standard "local" constitutive equation (7.1). On the other hand, because of the simplifying assumption of randomly oriented spheroids placed within hard "security" spheres, the related volume fractions are quite small for these extreme aspect ratio cases. In the limit $w \to 0/\infty$, the numerical results approach the vanishing analytical estimates obtained for disk/needle-shaped inclusions/voids. Figs. 5 and 6 show that for w in the ranges $w < 0.5$ and $w > 1.4$, the model used in the present paper becomes inadequate and a more sophisticated approach must be adopted, as discussed in Section 6.2.

Acknowledgements

Support by the University of Genoa and the Italian Ministry of Instruction, University and Research (MIUR), within a project promoting scientific activity of young researchers, is gratefully acknowledged. IM would also like to express particular thanks to Professor G. Emmert, Head of the Department of Engineering Physics, University of Wisconsin - Madison for the excellent working conditions provided during her

year-long visit as Visiting Scholar in 2000/2001. WJD gratefully acknowledges support from the National Science Foundation, Mechanics and Materials Program, Grant CMS-0136986.

Appendix A. Expected value of the intersection volume of two aligned spheroids randomly oriented

The two spheroids of semi-axes $a_1 = a_2 \neq a_3 = wa_1$ being aligned (Fig. 7a), this task can be made reasonable by performing a scale transformation, say from reference coordinates x_i to $X_i = x_i a/a_i$, so that the spheroids are converted into spheres of equal radius, say a. Thus, the problem reduces to an equivalent one involving two spheres, whose centers are a distance, say, R from one another (Fig. 7b).

It is then straightforward to show that, whatever the orientation, the intersection volume of two aligned spheroids is given by

$$V_{\text{int}} = \frac{a_1^2 a_3}{a^3} V_a \left(1 - \frac{3}{4}\frac{R}{a} + \frac{1}{16}\frac{R^3}{a^3}\right) \quad \text{when } 0 \leqslant R \leqslant 2a, \tag{A.1}$$

and $V_{\text{int}} = 0$ when $R > 2a$, with $V_a = 4/3\pi a^3$. From the scale transformation, the transformed radial coordinate R results in an angle-dependent center-to-center distance which can be expressed as follows:

$$R = \sqrt{X_1^2 + X_2^2 + X_3^2} = a\sqrt{\frac{x_1^2}{a_1^2} + \frac{x_2^2}{a_2^2} + \frac{x_3^2}{a_3^2}}$$

$$= \frac{ra}{a_3}\sqrt{w^2 \sin^2\theta + \cos^2\theta} \quad \text{with } 0 \leqslant \theta \leqslant \pi, \tag{A.2}$$

having introduced spherical coordinates (r, θ, ϕ) centered at one spheroid (Fig. 7a).

Now, in order to evaluate the expected value $\bar{V}_{\text{int}}$ of V_{int} over all possible orientations the spheroids can take, notice that in spherical coordinates this is equivalent to

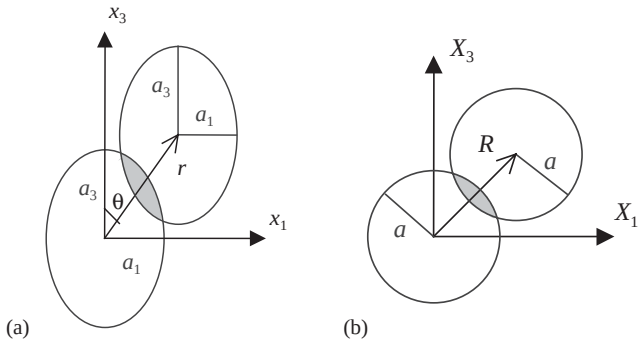

Fig. 7. Intersection volume of two aligned spheroids: (a) in reference coordinates **x** and (b) in transformed coordinates **X**.

averaging (A.1) combined with Eq. (A.2) over a spherical shell of fixed radius r:

$$\bar{V}_{\text{int}}(r) = \frac{1}{4\pi}\int_0^{2\pi}\int_0^{\pi} V_{\text{int}} \sin\theta \, \mathrm{d}\theta \, \mathrm{d}\phi. \tag{A.3}$$

The result is a function of r that $=0$ when $r > 2a$ and can be written for compactness as

$$\bar{V}_{\text{int}}(r) = V_a f_A(\rho)\chi_{2a}(r), \tag{A.4}$$

having introduced the indicator function $\chi_{2a}(r) = 1$ when $r \leqslant 2a$, and $=0$ otherwise; function $f_A(\rho)$ with $\rho = r/a$ must be specialized to the specific shape of the spheroids.

After integrating Eq. (A.3) for oblate spheroids ($a_1 = a,\ a_3 = wa,\ w \leqslant 1$), one obtains

$$f_A(\rho) = w \begin{cases} 1 + \dfrac{\rho(2\rho^2 + 3\rho^2 w^2 - 48w^2)}{128w^3} \\ \quad -\mathfrak{h}_o(\rho)\,\text{arcsinh}(\sqrt{1-w^2}/w), \quad 0 \leqslant \rho \leqslant 2w, \\ \dfrac{3(8+\rho^2)w}{64\rho}\sqrt{\dfrac{4-\rho^2}{1-w^2}} \\ \quad -\mathfrak{h}_o(\rho)\,\text{arcsinh}(\sqrt{4-\rho^2}/\rho), \quad 2w < \rho \leqslant 2, \end{cases} \tag{A.5}$$

having defined

$$\mathfrak{h}_o(\rho) = \frac{3\rho w(16-\rho^2)}{128\sqrt{1-w^2}}. \tag{A.6}$$

Analogously, for prolate spheroids ($a_1 = a/w,\ a_3 = a,\ w \geqslant 1$) there results

$$f_A(\rho) = \frac{1}{w^2}\begin{cases} \mathfrak{h}_{p1}(\rho), & 0 \leqslant \rho \leqslant 2/w, \\ \mathfrak{h}_{p1}(\rho) + \mathfrak{h}_{p2}(\rho) - \dfrac{3(8+\rho^2 w^2)}{64\rho}\sqrt{\dfrac{\rho^2 w^2 - 4}{w^2-1}}, & 2/w < \rho \leqslant 2, \end{cases} \tag{A.7}$$

where

$$\mathfrak{h}_{p1}(\rho) = 1 + \frac{\rho(2\rho^2 + 3\rho^2 w^2 - 48)}{128} - \frac{3\rho w^2(16-\rho^2 w^2)}{128\sqrt{w^2-1}}\,\text{arcsin}(\sqrt{w^2-1}/w), \tag{A.8}$$

and

$$\mathfrak{h}_{p2}(\rho) = \frac{3\rho w^2(16-\rho^2 w^2)}{128\sqrt{w^2-1}}\,\text{arcsin}(\sqrt{\rho^2 w^2 - 4}/\rho w). \tag{A.9}$$

It can be shown that, using $b = 1/w$ instead of w and setting $a = 1$, Eq. (A.7) together with Eqs. (A.8) and (A.9) gives precisely the expression found by Quintanilla (1999) for $b \leqslant 1$.

Eqs. (A.5) and (A.7) are now used to evaluate radial integrals (3.25) involving function f_A. After integrating Eq. (A.5) together with Eq. (A.6), for oblate spheroids we obtain

$$\mathfrak{F}_A = w^2 \frac{32\pi - 135\arcsin(w) + 71\arctan(w/\sqrt{1-w^2})}{160\sqrt{1-w^2}} \quad (w \leqslant 1), \tag{A.10}$$

and

$$\bar{\mathfrak{F}}_A = 3w^2 \frac{16\pi + 32w\sqrt{1-w^2} - 175\arcsin(w) + 143\arctan(w/\sqrt{1-w^2})}{560\sqrt{1-w^2}}$$

$$(w \leqslant 1). \tag{A.11}$$

For prolate spheroids, analogously, integrating Eq. (A.7) together with Eqs. (A.8) and (A.9) gives

$$\mathfrak{F}_A = \frac{2\ln(w + \sqrt{w^2-1})}{5w^3\sqrt{w^2-1}} \quad (w \geqslant 1), \tag{A.12}$$

and

$$\bar{\mathfrak{F}}_A = \frac{6}{35w^5}\left[w + \frac{\ln(w + \sqrt{w^2-1})}{\sqrt{w^2-1}}\right] \quad (w \geqslant 1). \tag{A.13}$$

Appendix B. Intersection volume of two inhomogeneous spheres

As noted in Section 3, one of the key points in the formulation is the geometrical interpretation of certain convolutions as intersection volumes of inhomogeneous spheres. A useful approach for their evaluation is suggested here.

Two inhomogeneous spheres of radii b and $\bar{b} \geqslant b$ and densities f and $\bar{f}$, respectively, have centers separated by d. It is straightforward that the two spheres intersect only if their centers are a distance $d < \bar{b} + b$ apart. If so, the related intersection volume V_{int} can be regarded as a function of d. Three situations in particular can occur; Fig. 8 shows these.

In order to evaluate V_{int}, spherical coordinates (r, ϕ, θ) centered at the lower sphere and spherical radial coordinate $\bar{r}$ centered at the upper sphere are introduced. Note that $\bar{r}$ is related to r by

$$\bar{r}^2 = r^2 - 2dr\cos\phi + d^2. \tag{B.1}$$

For $\boxed{\bar{b} \leqslant d < \bar{b} + b}$ (Fig. 8a), only a small upper portion of the lower sphere falls in the upper one. This portion corresponds to $0 \leqslant \phi \leqslant \bar{\phi}$ and $d - \bar{b} \leqslant r \leqslant b$, where $\bar{\phi}$

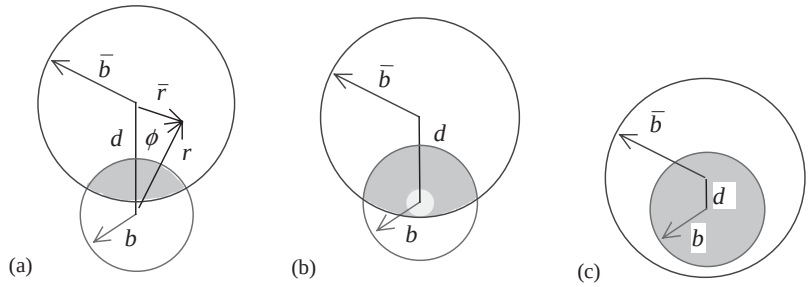

Fig. 8. Intersection of two spheres of radii b and $\bar{b} \geqslant b$: (a) for $\bar{b} \leqslant d < \bar{b} + b$; (b) for $\bar{b} - b < d < \bar{b}$; (c) for $0 \leqslant d \leqslant \bar{b} - b$.

follows directly from Eq. (B.1) having set $\bar{r} = \bar{b}$

$$\bar{\phi} = \arccos\left(\frac{r^2 + d^2 - \bar{b}^2}{2dr}\right). \tag{B.2}$$

The intersection volume can thus be written as:

$$V_{\text{int}} = \int_0^{2\pi} \left[\int_{d-\bar{b}}^{b} \int_0^{\bar{\phi}} f(r)\bar{f}(\bar{r}) r^2 \sin\phi \, \mathrm{d}\phi \, \mathrm{d}r\right] \mathrm{d}\theta. \tag{B.3}$$

Using Eq. (B.1) to substitute for $\bar{r}$ and noting that the integrand is independent of θ so that the θ-integral can be immediately evaluated, V_{int} yields:

$$V_{\text{int}} = 2\pi \int_{d-\bar{b}}^{b} r^2 f(r) \left(\int_0^{\bar{\phi}} \bar{f}(\sqrt{r^2 - 2dr\cos\phi + d^2}) \sin\phi \, \mathrm{d}\phi\right) \mathrm{d}r. \tag{B.4}$$

For $\boxed{\bar{b} - b < d < \bar{b}}$ (Fig. 8b), most of the lower sphere falls in the upper one. In this case intersection points are characterized by: $0 \leqslant \phi \leqslant \pi$ when $0 \leqslant r \leqslant \bar{b} - d$ and $0 \leqslant \phi \leqslant \bar{\phi}$ when $\bar{b} - d < r \leqslant b$, $\bar{\phi}$ always given by Eq. (B.2). Analogously to the previous case, the intersection volume is now given by:

$$\begin{aligned} V_{\text{int}} = {} & 2\pi \int_0^{\bar{b}-d} r^2 f(r) \left(\int_0^{\pi} \bar{f}(\sqrt{r^2 - 2dr\cos\phi + d^2}) \sin\phi \, \mathrm{d}\phi\right) \mathrm{d}r \\ & + 2\pi \int_{\bar{b}-d}^{b} r^2 f(r) \left(\int_0^{\bar{\phi}} \bar{f}(\sqrt{r^2 - 2dr\cos\phi + d^2}) \sin\phi \, \mathrm{d}\phi\right) \mathrm{d}r. \end{aligned} \tag{B.5}$$

For $\boxed{0 \leqslant d \leqslant \bar{b} - b}$ (Fig. 8c), the entire lower sphere falls in the upper one. Thus, the intersection volume is simply:

$$V_{\text{int}} = 2\pi \int_0^{b} r^2 f(r) \left(\int_0^{\pi} \bar{f}(\sqrt{r^2 - 2dr\cos\phi + d^2}) \sin\phi \, \mathrm{d}\phi\right) \mathrm{d}r. \tag{B.6}$$

The formulation can be straightforwardly specialized to cases involving only one inhomogeneous sphere, say the lower one. As an example, setting $\bar{f}(\bar{r}) = 1$ in Eqs. (B.4)–(B.6) and evaluating ϕ-integrals, it follows immediately that

$$V_{\text{int}} = \begin{cases} 4\pi \displaystyle\int_0^b r^2 f(r)\,\mathrm{d}r, & 0 \leqslant d \leqslant \bar{b} - b, \\ 4\pi \displaystyle\int_0^{\bar{b}-d} r^2 f(r)\,\mathrm{d}r + \pi \int_{\bar{b}-d}^b \frac{r[\bar{b}^2 - (d-r)^2]}{d} f(r)\,\mathrm{d}r, & \bar{b} - b < d < \bar{b}, \\ \pi \displaystyle\int_{d-\bar{b}}^b \frac{r[\bar{b}^2 - (d-r)^2]}{d} f(r)\,\mathrm{d}r, & \bar{b} \leqslant d < \bar{b} + b, \end{cases} \tag{B.7}$$

which can be further specialized to the case of identical spheres ($\bar{b} = b$):

$$V_{\text{int}} = \begin{cases} 4\pi \displaystyle\int_0^{b-d} r^2 f(r)\,\mathrm{d}r + \pi \int_{b-d}^b \frac{r[b^2 - (d-r)^2]}{d} f(r)\,\mathrm{d}r, & 0 \leqslant d < b, \\ \pi \displaystyle\int_{d-b}^b \frac{r[b^2 - (d-r)^2]}{d} f(r)\,\mathrm{d}r, & b \leqslant d < 2b. \end{cases} \tag{B.8}$$

These results are used in Section 3 where the partial derivative with respect to $\bar{b}$ of Eq. (B.7) is also employed. It is derived here and yields:

$$\frac{\partial V_{\text{int}}}{\partial \bar{b}} = \begin{cases} 0, & 0 \leqslant d \leqslant \bar{b} - b, \\ 2\pi \displaystyle\int_{\bar{b}-d}^b \frac{r\bar{b}}{d} f(r)\,\mathrm{d}r, & \bar{b} - b < d < \bar{b}, \\ 2\pi \displaystyle\int_{d-\bar{b}}^b \frac{r\bar{b}}{d} f(r)\,\mathrm{d}r, & \bar{b} \leqslant d < \bar{b} + b. \end{cases} \tag{B.9}$$

References

Atkinson, K.E., 1989. An Introduction to Numerical Analysis. Wiley, Singapore.

Drugan, W.J., 2000. Micromechanics-based variational estimates for a higher-order nonlocal constitutive equation and optimal choice of effective moduli for elastic composites. J. Mech. Phys. Solids 48, 1359–1387.

Drugan, W.J., Willis, J.R., 1996. A micromechanics-based nonlocal constitutive equation and estimates of representative volume element size for elastic composites. J. Mech. Phys. Solids 44, 497–524.

Hashin, Z., Shtrikman, S., 1962a. On some variational principles in anisotropic and nonhomogeneous elasticity. J. Mech. Phys. Solids 10, 335–342.

Hashin, Z., Shtrikman, S., 1962b. A variational approach to the theory of the elastic behaviour of polycrystals. J. Mech. Phys. Solids 10, 343–352.

Høye, J.S., Stell, G., 1976. Configurationally disordered spin systems. Phys. Rev. Lett. 36, 1569–1573.
Markov, K.Z., 1998. On the cluster bounds for the effective properties of microcracked solids. J. Mech. Phys. Solids 46, 357–388.
Markov, K.Z., Willis, J.R., 1998. On the two-point correlation function for dispersions of nonoverlapping spheres. Math. Models Methods Appl. Sci. 8, 359–377.
Percus, J.K., Yevick, G.J., 1958. Analysis of classical statistical mechanics by means of collective coordinates. Phys. Rev. 110, 1–13.
Ponte Castañeda, P., Willis, J.R., 1995. The effect of spatial distribution on the effective behavior of composite materials and cracked media. J. Mech. Phys. Solids 43, 1919–1951.
Quintanilla, J., 1999. Microstructure functions for random media with impenetrable particles. Phys. Rev. E 60, 5788–5794.
Rintoul, M.D., Torquato, S., 1996. Computer simulations of dense hard-sphere systems. J. Chem. Phys. 105, 9258–9265.
Torquato, S., Stell, G., 1985. Microstructure of two-phase random media. V. The *n*-point matrix probability functions for impenetrable spheres. J. Chem. Phys. 82, 980–987.
Verlet, L., Weis, J.J., 1972. Equilibrium theory of simple liquids. Phys. Rev. A 5, 939–952.
Wertheim, M.S., 1963. Exact solution of the Percus-Yevick integral equation for hard spheres. Phys. Rev. Lett. 10, 321–323.
Willis, J.R., 1977. Bounds and self-consistent estimates for the overall properties of anisotropic composites. J. Mech. Phys. Solids 25, 185–202.
Willis, J.R., 1982. Elasticity theory of composites. In: Hopkins, H.G., Sewell, M.J. (Eds.), Mechanics of Solids: The R. Hill 60th Anniversary Volume. Pergamon Press, Oxford, pp. 653–686.
Willis, J.R., 1983. The overall elastic response of composite materials. ASME J. Appl. Mech. 50, 1202–1209.